Smart Energy 1 (2021) 100009

Contents lists available at ScienceDirect

Smart Energy

journal homepage: www.journals.elsevier.com/smart-energy

On the correlation between building heat demand and wind energy supply and how it helps to avoid blackouts

Mark Z. Jacobson

Department of Civil and Environmental Engineering, Stanford University, Stanford, CA, 94305-4020, USA

ARTICLE INFO

Article history:
Received 29 September 2020
Received in revised form
2 March 2021
Accepted 2 March 2021
Available online 5 March 2021

Keywords:
Renewable energy
Grid stability
Building energy
Heat loads
Wind energy
Weather

ABSTRACT

Keeping the electric and heat grids stable is the major challenge facing the world as it transitions away from fossil fuels to electricity and heat provided by wind, water, and sunlight (WWS). Because building heating and cooling demands and wind and solar energy supplies both depend on the same weather, building demands should be modeled consistently with renewable supplies. However, no model to date has calculated future thermal loads consistently with future renewable supplies. Here, a global weather/climate model is used to do this. Grid stability in 24 world regions encompassing 143 countries is then examined. Low cost solutions are found everywhere. Building heat loads are found to correlate strongly with wind energy supply aggregated over large, cold regions. Moderate correlations are found elsewhere, except no correlation is found in some tropical islands and some small countries. Thus, wind energy in most climates can help to meet seasonal heat loads, thereby helping to reduce the cost of energy. Finally, wind and solar power supplies are negatively correlated, indicating that wind and solar are complementary in nature and should both be built, where feasible, to reduce output variability arising from installing only one of them.
© 2021 The Author(s). Published by Elsevier Ltd. This is an open access article under the CC BY-NC-ND license (http://creativecommons.org/licenses/by-nc-nd/4.0/).

In order to reduce substantially or eliminate the seven million annual air pollution deaths, global warming, and energy insecurity that arise from fossil fuel use, the world is transitioning all energy sectors toward clean, renewable electricity and heat. However, a major concern is whether heat demand in buildings can be met every minute with renewable electricity and direct heat supply. An additional question is whether all energy demand can be met every minute with clean, renewable electricity and heat supply. This study addresses both issues. It first uses a global weather-climate model to simulate future building heat and cold demands worldwide consistently with wind and solar supply. In doing so, it finds a strong positive correlation between wind supply, aggregated over large, cold regions, and building heat demand in the same regions. It also finds weak negative correlations between wind supply and building cold demand and between wind supply and solar supply. The latter anticorrelation suggests wind and solar supplies are complementary in nature. Finally, the data are used to find low-cost solutions to grid stability in 24 world regions encompassing 143 countries. The study concludes that, due to the strong correlation between wind supply and heat demand, wind energy in most climates can help to meet seasonal heat demand while reducing the cost of energy.

1. Introduction

Many studies have examined the feasibility of matching electricity and/or heat demand with supply, storage, and/or demand response upon transitioning one or more energy sectors entirely to 100% renewable energy. Some of these studies quantified installations needed to match annual-average demand among all energy sectors (electricity, buildings, transportation, industry, etc.) worldwide or in most countries with renewable supply [1,2]. Others quantified installations needed to meet demand continuously worldwide among all energy sectors [3–5]; in one country in the electric power sector [6–15], in one country among multiple energy sectors [16–22]; on the continental scale in the electric power sector [23,24], or on the continental scale among multiple sectors [25,26].

Studies that treated multiple sectors assumed that heating was electrified through the use of either electric heat pumps or resistance heating. Some studies that treated the electrification of heating also considered district heating and/or energy efficiency/weatherization measures to reduce heat demand in buildings. All

E-mail address: jacobson@stanford.edu.

https://doi.org/10.1016/j.segy.2021.100009
2666-9552/© 2021 The Author(s). Published by Elsevier Ltd. This is an open access article under the CC BY-NC-ND license (http://creativecommons.org/licenses/by-nc-nd/4.0/).

three measures (electrification of heat, district heating, and efficiency in buildings) are important for providing continuous energy with 100% renewables [27–29]. The main conclusion among all the studies discussed is that such a transition, while facing social and political challenges, is economically beneficial from both a business and social cost point of view.

However, future-year modeling scenarios of matching demand with supply, storage, and demand response have been limited by the inconsistency between time-series datasets of wind and solar supply and of building thermal (heating and cooling) demand. For example, Olsen et al. [30] modeled building hourly heating and cooling loads in California using pre-existing local temperature data. However, they did not simultaneously model solar or wind fields. Hale et al. [31] similarly used past meteorological data at 30-min or hourly resolution to model building heating and cooling loads but did not model future years nor solar or wind fields. Toktarova et al. [32] and Bogdanov et al. [21] used 2005 temperature data to estimate air conditioning loads and 2005 heating degree day data to estimate heat loads at an hourly resolution. Bogdanov et al. [5] used 2005 satellite data to produce hourly solar and wind fields and followed the method of Toktarova et al. [32] (using heating degree day and temperature data) to derive heat and air conditioning loads based on 2005 data. None of these studies predicted future (rather than past) renewable energy supply consistently with building heating and cooling loads, particularly at a 30-s resolution. Whereas thermal loads for buildings generally do not vary so much over 30 s, wind and solar electricity production can.

This study fills that gap by modeling future wind and solar radiation fields consistently in time and space with building heating and cooling loads through the use of a global weather-climate-air pollution model. Such fields are then applied to look at correlations among wind output, solar output, and thermal loads and to study grid stability in 24 world regions encompassing 143 countries at 30-s time resolution with a grid integration model.

2. Methods

This study uses a grid integration model, LOADMATCH [3,4,19], to simulate matching electricity and heat demand with supply and storage over time. LOADMATCH requires time-dependent intermittent demand (load) profiles; wind-water-solar (WWS) electricity and heat supply profiles; supply and characteristics of storage, demand response and transmission/distribution as inputs.

Demand in the model is summed across all energy sectors (the residential, commercial, transportation, industrial, agricultural/forestry/fishing, and military sectors) after all sectors have been converted so that their energy originates or from electricity or direct low-temperature heat.

Electricity in the model comes from only WWS electricity sources (Wind: onshore and offshore wind turbines; Water: hydroelectric plants, geothermal plants, wave devices, tidal turbines; and Solar: residential and commercial/government rooftop PV, utility PV, and CSP). Direct low-temperature heat comes from WWS heat sources (solar and geothermal heat).

Electricity in LOADMATCH powers electric heat pumps for low-temperature heat (beyond the heat supplied by direct geothermal or solar thermal heat) and air conditioning. Electricity also powers high-temperature heat for industrial processes, battery-electric vehicles, electrolytic hydrogen for hydrogen fuel cell electric vehicles (for long-distance, heavy transport), and all electric appliances, equipment, and machines.

For this study, LOADMATCH was updated to include, as inputs, time-dependent heating and cooling loads determined consistently with time-dependent WWS generation. Previously, heating and cooling loads were estimated using heating- and cooling-degree day data from past years. Such data were not consistent with the future estimates of wind and solar data modeled in those prior studies and were available only at a daily resolution.

Both wind and solar electricity and heat generation and thermal loads are calculated here every 30 s in 2050 with the global weather-climate-air-pollution model, GATOR-GCMOM (Gas, Aerosol, Transport, Radiation, General Circulation, Mesoscale, and Ocean Model) [33–36]. This model predicts time- and spatially-distributed meteorological fields (wind, temperature, pressure, humidity, size- and composition-resolved clouds), radiative fields (spectral solar and thermal infrared radiation, heating rates, and actinic fluxes), gas processes (emissions, gas photochemistry, gas transport, gas-to-particle conversion, gas-cloud interactions, and gas removal), aerosol processes (emissions, homogeneous nucleation, coagulation, condensation, dissolution, equilibrium and non-equilibrium chemistry, aerosol-cloud interactions, and aerosol removal), and cloud processes (activation, collision-coalescence, condensation/evaporation, dissolution, drop breakup, ice formation, graupel formation, lightning, convection within, and precipitation), and more. In addition, GATOR-GCMOM simulates feedbacks among meteorology, solar and thermal-infrared radiation, gases, aerosol particles, cloud particles, oceans, sea ice, snow, soil, and vegetation. Model predictions have been compared with data in 34 peer-reviewed studies. The model has also taken part in 14 model inter-comparisons [3].

In terms of WWS supply, GATOR-GCMOM predicts time- and space-dependent electricity production from onshore and offshore wind, rooftop and utility scale PV, and CSP. It also predicts solar-thermal heat production. From the wind data, time-dependent fields of wave power are also derived.

GATOR-GCMOM accounts for the reduction in the wind's kinetic energy and speed due to the competition among wind turbines for limited available kinetic energy [35], the temperature-dependence of PV output [36], and the reduction in direct and diffuse sunlight to building and the ground due to conversion of radiation to electricity by solar devices [3,4]. It also accounts for (1) changes in air and ground temperature due to power extraction by solar and wind devices and subsequent electricity use [3,4]; (2) impacts of time-dependent gas, aerosol, and cloud concentrations on solar radiation and wind fields [34]; (3) radiation to rooftop PV panels at a fixed optimal tilt at their location [36]; and (4) radiation to utility PV panels, half of which are at an optimal tilt and the other half of which track the sun with single-axis horizontal tracking [36].

For this study, GATOR-GCMOM was updated to predict building heating and cooling loads in each country c in each surface grid cell (i,j, where $i = 1$. the number of east-west cells and $j = 1$ to the number south-north cells), and for each 30-s dynamical time step t. Each model surface grid cell can contain any number of countries, depending on the horizontal resolution of the cell. The thermal heating (negative) or cooling (positive) load ($L_{thermal}$, W) required to maintain a constant indoor temperature is

$$L_{\mathrm{thermal,i,j,c,t}} = (T_{\mathrm{i,j,t}} - T_{\mathrm{ref}}) \times A \times U \times N_{B,\mathrm{i,j,c}} \quad (1)$$

where T is ambient temperature in the grid cell (predicted by GATOR-GCMOM), T_{ref} is the desired building interior temperature, which is variable but was set to 294.261 K (70 °F) for this study, A is the surface area (m^2) of an average building (Table S1), U is the average U-value (W/m [2]-K) of the average building (Table S1), and N_B is the number of average-sized buildings in country c within the grid cell. The number of buildings in a country in each grid cell is estimated from the population in the country in the grid cell divided by the average number of residents in a household, all multiplied by the ratio of residential plus commercial building floor

area to residential building floor area. For example, the U.S. has an average of 2.36 residents per household and a residential plus commercial floor area to residential floor area ratio of 1.26. For simplicity, these numbers were used here in all countries. The exact value of the number of buildings or residents per building in each country is not so important, because the resulting thermal loads from GATOR-GCMOM are used only to distribute LOADMATCH annual-average thermal loads over time rather than to determine their magnitude. The spatial distribution of population, thus the distribution of buildings, is more important since thermal loads vary by location in a country. This is accounted for in GATOR-GCMOM.

Each 30-s time step, the modeled loads from Equation (1) are summed among all surface grid cells in each country to give country totals. As such, spatial differences in heating requirements due to differences in outdoor temperature across a country, even one that spans multiple time zones, are accounted for each time step. Country total heating and cooling loads are written to a file every 30 s along with modeled instantaneous power output from onshore and offshore wind, solar rooftop PV, utility scale PV, CSP, and solar thermal heat.

LOADMATCH is a trial-and-error simulation model. It works by running multiple simulations, one at a time. Each simulation marches one or more years, one timestep at a time, just as the real world does. The main constraint during a simulation is that the summed electricity, heat, cold, and hydrogen load, adjusted by demand response, must match energy supply and storage every timestep for an entire simulation period. If load is not met during any timestep, the simulation stops. Inputs (either the nameplate capacity of one or more generators; the peak charge rate, peak discharge rate, or peak capacity of storage; or characteristics of demand response) are then adjusted one at a time based on an examination of what caused the load mismatch (hence the description “trial-and-error” model). For example, if hydrogen or underground thermal energy storage is full when a mismatch occurs, a solution is to increase slightly the storage capacity of the one that is full. In cases where the cause is uncertain, generator nameplate capacities and storage peak discharge rates are increased one generator and one storage device at a time. Each update, another simulation is run from the beginning. New simulations are run until load is met every time step of the simulation period. After load is met once, additional simulations are performed with further-adjusted inputs to generate a set of lower-cost solutions that match load every timestep. The lowest cost solution among all successful simulations is then selected.

The wind and solar power supplies in GATOR-GCMOM are modeled using the initial estimated nameplate capacities by country used in LOADMATCH. As nameplate capacities in LOADMATCH are adjusted each simulation based on the methodology just described, time-dependent WWS supplies from GATOR-GCMOM are scaled proportionately to ensure a consistency between WWS supply from GATOR-GCMOM and nameplate capacities assumed in LOADMATCH.

Unlike with an optimization model, which solves among all timesteps simultaneously, a trial-and-error model does not know what the weather will be during the next timestep. Because a trial-and-error model is non-iterative, it requires less than a minute for a 3-year simulation with a 30-s timestep [3]. This is 1/500th to 1/100,000th the computer time of an optimization model for the same number of timesteps. The disadvantage of a trial-and-error model compared with an optimization model is that the former does not determine the least cost solution out of all possible solutions. Instead, it produces a set of viable solutions, from which the lowest-cost solution is selected.

Table S2 summarizes many of the processes treated in LOADMATCH. Model inputs are as follows: (1) time-dependent electricity produced from onshore and offshore wind turbines, wave devices, tidal turbines, rooftop PV panels, utility PV plants, CSP plants, and geothermal plants; (2) a hydropower peak discharge rate (nameplate capacity), which is set to the present-day hydropower nameplate capacity for each region, a hydropower mean recharge rate (from rainfall), and a hydropower annual average electricity output (which is near the current output); (3) time-dependent geothermal heat and solar-thermal heat generation rates; (4) specifications of hot-water and chilled-water sensible-heat thermal energy storage (HW-STES and CW-STES) (peak charge rate, peak discharge rate, peak storage capacity, losses into storage, and losses out of storage); (5) specifications of underground thermal energy storage (UTES), including borehole, water pit, and aquifer storage; (6) specifications of ice storage (ICE); (7) specifications of electricity storage in pumped hydropower storage (PHS), phase-change materials coupled with CSP (CSP-PCM), and batteries; (8) specifications of hydrogen (for use in transportation) electrolysis, compression, and storage equipment; (9) specifications of electric heat pumps for air and water heating and cooling; (10) specifications of a demand response system; (11) specifications of losses along short- and long-distance transmission and distribution lines; (12) time-dependent electricity, heat, cold, and hydrogen loads, and (13) scheduled and unscheduled maintenance downtimes for generators, storage, and transmission.

One assumption here is that transmission is perfectly interconnected in each grid region. Whereas the study accounts for transmission and distribution costs and losses, it assumes that electricity can flow to where it is needed without bottlenecks. This concern applies to only about half the regions examined since 11 regions (Iceland, Cuba, Jamaica, Haiti/Dominican Republic, Israel, Japan, Mauritius, New Zealand, Philippines, South Korea, and Taiwan) have or could have, due to their small sizes, well-connected transmission and distribution systems. Stable, low-cost systems were found here for all those regions. As such, there is no reason to think that the United States, for example, broken up into multiple isolated or moderately-interconnected regions versus one completely-interconnected region can’t also maintain a low-cost, stable 100% WWS grid. In fact, many of the dozens of papers that have examined 100% renewable grids have treated transmission spatially and have found low-cost solutions. Aghahosseini et al. [26], for example, found stable, low-cost, time-dependent electric grid solutions when each North and South America were run on 100% renewables, and transmission flows were modeled explicitly among multiple lines. While the present paper sacrifices spatial resolution needed to treat transmission explicitly, it treats time resolution (30 s) higher than other studies. This study also accounts for the spatial variation in wind and solar resources and thermal loads within large countries.

Next, the order of operations in LOADMATCH, including how the model treats excess generation over demand and excess demand over generation, is summarized. The first situation discussed is one in which the current (instantaneous) supply of WWS electricity or heat exceeds the current electricity or heat demand (load). The total load, whether for electricity or heat, consists of flexible and inflexible loads. Whereas flexible loads may be shifted forward in time with demand response, inflexible loads must be met immediately. If WWS instantaneous electricity or heat supply exceeds the instantaneous inflexible electricity or heat load, then the supply is used to satisfy that load. The excess WWS is then used to satisfy as much current flexible electric or heat load as possible. If any excess electricity exists after inflexible and current flexible loads are met, the excess electricity is sent to fill electricity, heat, cold, or hydrogen storage.

Electricity storage is filled first. Excess CSP high-temperature

heat goes to CSP thermal energy storage in a phase-change material. If CSP storage is full, remaining high-temperature heat produces electricity that is used, along with excess electricity from other sources, to charge pumped hydropower storage followed by battery storage, cold water storage, ice storage, hot water tank storage, and underground thermal energy storage. Remaining excess electricity is used to produce hydrogen. Any residual after that is shed.

Heat and cold storage are filled by using the excess electricity to run an air source or ground source heat pump to move heat or cold from the air, water, or ground to the thermal storage medium. Hydrogen storage is filled by using electricity for an electrolyzer to produce hydrogen and for a compressor to compress the hydrogen, which is then moved to a storage tank.

If any excess direct geothermal or solar heat exists after it is used to satisfy inflexible and flexible heat loads, the remainder is used to fill either district heat storage (water tank and underground heat storage) or building hot water tank heat storage.

The second situation discussed is one in which current load exceeds WWS electricity or heat supply. When current inflexible plus flexible electricity load exceeds the current WWS electricity supply from the grid, the first step is to use electricity storage (CSP, pumped hydro, hydropower, and battery storage, in that order) to fill in the gap in supply. The electricity is used to supply the inflexible load first, followed by the flexible load.

If electricity storage becomes depleted and flexible load persists, demand response is used to shift the flexible load to a future hour.

If the inflexible plus flexible heat load subject to storage exceeds WWS direct heat supply, then stored district heat (in water tanks and underground storage) is used to satisfy district heat loads subject to storage, and stored building heat (in hot water tanks) is used to satisfy building water heat loads. If stored heat becomes exhausted, then any remaining low-temperature air or water heat load becomes either an inflexible load (85%), which must be met immediately with electricity, or a flexible load (15%), which can either be met with electricity or shifted forward in time with demand response and turned into an inflexible load.

Similarly, if the inflexible plus flexible cold load subject to storage exceeds cold storage (in ice or water), excess cold load becomes either an inflexible load (85%), which must be met immediately with electricity, or a flexible load (15%), which can be met with electricity or shifted forward in time with demand response and turned into an inflexible load.

Finally, if current hydrogen load depletes hydrogen storage, the remaining hydrogen load becomes an inflexible electrical load that must be met immediately with current electricity.

In any of the cases above, if electricity is not available to meet the remaining inflexible load, the simulation stops and must restart after nameplate capacities of generation and/or storage are increased.

Because the model does not permit load loss at any time, it is designed to exceed the utility industry standard of load loss once every 10 years.

Next, the modifications to the above treatment for this study are discussed. The primary building heating and cooling loads needed in LOADMATCH include loads for air and water heating, air conditioning, and refrigeration. These loads are further divided into inflexible loads, loads subject to storage (district heating storage and domestic hot water storage), and loads subject to demand response. Such loads are calculated in the same way as in Jacobson et al. [3], except for the following updates:

1) F_{max}, which is the maximum allowable fraction of building electric load that is for air conditioning, is increased from 0.4 to 0.8 to allow for greater maximum cooling loads in a couple of regions.
2) C and H are re-defined from the average number of cooling and heating degree days per year to the annual-average cooling and heating loads obtained from GATOR-GCMOM. Table 1 provides values of C and H for each world region.
3) The fraction of total residential and commercial energy load that is heat load (F_h, defined in Equation S6 of Ref. 3) is recalculated assuming electric heat pumps provide all heat (Table S3).
4) The fraction of heating and cooling load subject to district heating was updated for some countries (Table S4).
5) The annual average regional building heat load in LOADMATCH is now scaled each LOADMATCH times step (30 s) with output from GATOR-GCMOM rather than scaled each day with heating degree day data. The new time-dependent regional heating load (GW) used in LOADMATCH during time step t is

$$L_{heat,t} = L_{heat} H_t / H \quad (2)$$

where L_{heat} is the annual average regional heat load (GW) used in LOADMATCH (Table 1), H_t is the heat load (GW) during time step t from GATOR-GCMOM, and H is the annual average heat load (GW) from GATOR-GCMOM (Table 1). To ensure at least some heat is distributed each time step of the year for water heating even in cases where air heating loads are limited to very few hours per year, a minimum heat load is calculated as $h \sum H_t / [F \sum h]$, where $h = 30$ s is the time step size, each summation is over all time steps in a year, and $F = 30$ if the fraction of all times steps where $H_t > 0$ during the year exceeds 0.3; $F = 10$ if the fraction is 0.1–0.3; $F = 1$ if it is 0.01–0.1, and $F = 0.01$ otherwise. This allows for water heating to occur in buildings even if no air heating is needed.

Footnote. The total cold and heat loads consist of flexible cold and heat loads subject to storage, flexible cold and heat loads not subject to storage, and inflexible cold and heat loads.

The instantaneous heat load is then partitioned into instantaneous heat loads subject to storage and not subject to storage, respectively, with

$$L_{heat,\ stor,t} = L_{heat,\ stor} L_{heat,t} / L_{heat} \quad (3)$$

$$L_{heat,\ nostor,t} = L_{heat,t} - L_{heat,\ stor,t} \quad (4)$$

Where $L_{heat,\ stor}$ is calculated as in Jacobson et al. [3]. Fifteen percent of the heat load not subject to storage is treated as flexible and subject to demand response in all sectors [3]. The rest is treated as inflexible.

Similarly, each region's annually averaged total cooling load (L_{cold}, GW) in LOADMATCH (Table 1) is converted to a time-dependent cooling load each LOADMATCH time step t with

$$L_{cold,t} = L_{cold} C_t / C \quad (5)$$

where C_t is the cold load (GW) during time step t from GATOR-GCMOM, and C is the annual average cold load (GW) from GATOR-GCMOM (Table 1). A minimum cold load for refrigeration is established each time step, just as for heating. The time-dependent total cold load is then partitioned into a time-dependent cold load subject to storage and not subject to storage, respectively, with

$$L_{cold,\ stor,t} = L_{cold,\ stor} L_{cold,t} / L_{cold} \quad (6)$$

$$L_{cold,\ nostor,t} = L_{cold,t} - L_{cold,\ stor,t} \quad (7)$$

The cold load not subject to storage is then treated as 15% flexible and subject to demand response in all sectors and the rest,

Table 1
a) 2050 annual average end-use electric plus heat load (GW) by region after energy in all sectors has been converted to WWS electricity or direct heat. Instantaneous loads can be higher or lower than annual average loads; b) end-use energy consumed during the one-year simulation (= end-use load x 8747.4875 h/simulation, from Table S17); c) total annual average building cold load (for air cooling and refrigeration) in LOADMATCH assuming a realistic penetration of cooling systems; d) total annual average building heat load (for air and water heating) in LOADMATCH assuming heating is provided by heat pumps running on electricity with a coefficient of performance of 4 and a realistic penetration of heating in buildings; e) fraction of hours of the year from GATOR-GCMOM during which a cold load arises; f) same for warm load; g) annual average cold load required to cool air in all buildings in each region, from GATOR-GCMOM; h) annual average heat load, required to warm air in all buildings in each region, before heat pumps are assumed; and i) fraction of air heat plus cold load that is cold load in GATOR-GCMOM.

Region	(a) Annual average total end-use load in LOAD-MATCH (GW)	(b) End-use energy used over simulation (TWh/sim)	(c) Total cold load (L_{cold}) in LOAD-MATCH (GW)	(d) Total heat load (L_{heat}) in LOAD-MATCH after it is converted to electricity for heat pumps (GW)	(e) Fraction of hours of year with cold load from GATOR-GCMOM	(f) Fraction of hours of year with heat load from GATOR-GCMOM	(g) Cold load (C) in GATOR-GCMOM for building air cooling only (GW)	(h) Heat load (H) in GATOR-GCMOM for building air heating only (GW)	(i) Fraction of annual heating + cooling load from GATOR-GCMOM that is cooling = C/(C + H)
Africa	482	4214	91.7	92.0	1	1	897	274	0.766
Australia	93.6	819	3.8	11.9	1	1	3.1	15.5	0.167
Canada	151	1326	2.4	25.2	0.338	1	2.2	74.9	0.029
Central America	154	1351	12.4	18.9	1	1	47.6	80.6	0.371
Central Asia	151	1322	24.9	26.0	0.957	1	219	182	0.546
China	2328	20,368	107	369	0.780	1	300	1411	0.175
Cuba	8.06	71	1.6	1.0	0.984	0.428	4.1	0.5	0.881
Europe	940	8220	20.8	200	0.617	1	42.1	707	0.056
Haiti	7.54	66	1.6	1.1	1	0.407	10.5	1.8	0.855
Iceland	2.98	26	0	0.4	0	1	0	0.7	0
India	945	8267	117	125	1	1	1291	222	0.853
Israel	12.8	112	0.7	2.1	0.511	0.929	1.7	6.3	0.211
Jamaica	2.27	20	0.2	0.1	0.994	0.051	1.9	0	0.985
Japan	178	1557	3.4	28.4	0.983	1	5.5	112	0.047
Mauritius	1.79	16	0.4	0.2	1	0.0011	0.8	0	0.992
Mideast	678	5928	58.7	91.5	1	1	177	311	0.363
New Zealand	17.6	154	0.2	2.1	0.211	1	0	3.8	0.006
Philippines	40.5	354	8.3	7.1	1	0.649	92.9	1.3	0.987
Russia	236	2068	4.6	65	0.450	1	9.4	281	0.032
South America	489	4278	71.7	47.8	1	1	174	128	0.577
Southeast Asia	583	5102	91.1	75.5	1	1	590	74.5	0.888
South Korea	155	1358	3.4	25	0.357	1	2.5	55.5	0.044
Taiwan	94.9	830	9.1	12.5	0.875	0.802	3.9	6.4	0.382
United States	939	8218	34.7	147	1	1	77.3	468	0.142
Total 2050	**8693**	76,042	**670**	**1375**			**3952**	**4417**	**0.472**

inflexible [3].

In sum, the total cooling and low-temperature heating loads in Table 1 are the sum of a flexible cooling and heating load subject to storage, a flexible cooling and heating load not subject to storage, and an inflexible cooling and heating load. All three types of annual-average cooling and heating loads are converted to a time series using data from GATOR-GCMOM. Table S4 shows the fractions of total heating and cooling load in each energy sector in each region that are applied to air heating, water, heating, air conditioning, and refrigeration.

2.1. Simulations

The global weather-climate-air-pollution model, GATOR-GCMOM, was run here on the global scale for 1 year (2050) at 1.5° × 1.5° horizontal resolution. Electricity produced by onshore and offshore wind turbines, rooftop and utility photovoltaics (PV), and concentrated solar power (CSP); heat from solar thermal devices; building air heating loads; and building air cooling loads were summed and output for each of 143 countries every 30 s for the year. Those results were fed into LOADMATCH, which was run for each of 24 world regions encompassing the 143 countries (Table S5) over the year.

Annual average 2050 end-use load, after electrification, by sector in each country for this study was taken from Jacobson et al. [3] Table 2 indicates that less total energy is needed with WWS than in the business-*as*-usual (BAU) case because electrification of all energy sectors lowers 2050 energy demand across all 143 countries, compared with BAU, by about 57.1%. Of this reduction, 38.3% points are due to the efficiency of using WWS electricity over combustion; 12.1% points are due to eliminating energy in the mining, transporting, and refining of fossil fuels; and 6.6% points are due to end-use energy efficiency improvements and reduced energy use beyond those in BAU. Of the 38.3% reduction due to the efficiency advantage of WWS electricity, 21.7% points are due to the efficiency advantage of WWS transportation, 3.4% points are due to the efficiency advantage of WWS electricity for industrial heat, and 13.2% points are due to the efficiency advantage of heat pumps [3]. Despite the reduction in demand, the intermittency of several WWS resources requires the need for electricity, heat, cold, and hydrogen storage and demand response management. Finally, more transmission lines are needed to transmit electricity short and long distances.

Footnote. WWS reduces the total annual average end-use load compared with BAU by 57.1%. Aggregate private energy cost (Columns f or g) equals annual average end use load (Column b or a) multiplied by the mean cost per unit energy (Column e or d) and by 8760 h per year. The load-weighted mean over all regions and range

Table 2
2050 regional annual-average end-use (a) BAU and (b) WWS loads; (c) present values of the mean total capital cost for new WWS electricity, heat, cold, and hydrogen generation and storage and long-distance transmission installed between today and 2050; mean levelized private costs of all (d) BAU and (e) WWS energy (¢/kWh-all-energy-sectors, averaged between today and 2050, in USD 2013); (f) mean aggregate WWS private (equals social) energy costs per year (2013 USD $billion/yr), and mean aggregate BAU (g) private energy cost, (h) health cost, (i) climate cost, and (j) total social cost per year (2013 USD $billion/yr).

Region	(a) Annual average BAU end-use load (GW)	(b) Annual average WWS end-use load (GW)	(c) Mean WWS Total capital cost ($tril 2013)	(d) Mean BAU (¢/kWh-all energy)	(e) Mean WWS (¢/kWh-all energy)	(f) Mean annual WWS all-energy private and social cost ($bil/yr)	(g) Mean annual BAU all-energy private cost ($bil/yr)	(h) Mean annual BAU health cost ($bil/yr)	(i) Mean annual BAU climate cost ($bil/yr)	(j) = g + h + i Mean annual BAU total social cost ($bil/yr)
Africa	1395	482	3.73	10.11	8.32	351	1236	3544	1601	6381
Australia	215	94	0.82	10.34	9.03	74.0	194	31	336	561
Canada	404	152	0.69	8.24	6.99	92.8	292	38	489	818
Central America	381	154	1.38	10.86	9.55	129	362	283	559	1205
Central Asia	431	151	1.34	10.14	8.83	117	383	906	589	1877
China	5167	2328	16.6	9.28	8.32	1697	4201	9620	7384	21,205
Cuba	14.4	8.06	0.10	11.98	12.13	8.57	15.1	33.5	29.1	77.8
Europe	2293	940	6.39	10.34	8.30	683	2076	1588	2723	6387
Haiti	18.3	7.54	0.09	11.37	12.09	7.99	18.2	32.4	24.7	75.3
Iceland	5.17	2.98	0.00	8.36	6.58	1.69	3.79	0.37	2.71	6.87
India	1886	945	10.6	9.62	10.05	832	1589	8003	3196	12,788
Israel	25.9	12.8	0.17	10.90	11.95	13.4	24.8	14.1	44.2	83.1
Jamaica	4.71	2.27	0.03	11.85	11.06	2.20	4.89	3.04	7.01	14.94
Japan	372	178	1.47	10.78	9.51	148	352	234	690	1276
Mauritius	4.59	1.79	0.02	11.13	11.41	1.79	4.48	2.99	4.74	12.2
Mideast	1470	678	6.12	11.55	9.06	538	1487	768	2627	4881
New Zealand	32.4	17.6	0.12	9.20	8.33	12.8	26.1	4.65	30.7	61.4
Philippines	90.8	40.5	0.41	10.59	9.46	33.5	84.2	604	167	856
Russia	743	236	1.66	10.18	8.20	170	662	539	1136	2337
South America	1136	489	3.68	8.93	8.85	380	889	670	1131	2690
Southeast Asia	1379	583	6.54	10.70	9.85	503	1293	2169	1770	5232
South Korea	317	155	1.98	10.14	12.2	166	281	93.5	491	865
Taiwan	167	94.9	1.00	9.27	10.82	90.0	136	77.0	322	535
United States	2303	939	7.83	10.43	9.20	757	2104	742	3067	5913
Total/ average	**20,255**	**8693**	**72.8**	**9.99**	**8.94**	**6809**	**17,719**	**30,001**	**28,419**	**76,140**

of the mean WWS cost per unit energy, is 8.93 (7.18−11.3) ¢/kWh-all energy. Table S6 gives the lifecycle costs and efficiencies of storage for each storage type. Tables S7−S9 give parameters for determining the costs of energy generation, health damage avoided, and climate damage avoided, respectively, with WWS. The discount rate used for generation, storage, transmission/distribution, and social costs is a social discount rate of 2 (1−3)% [3].

Annual average total 2050 WWS loads in each sector for each of 143 countries were obtained from Ref. 3, who first projected contemporary BAU loads to 2050 before they were converted to WWS loads. Table S10 summarizes the resulting 2050 WWS loads, separated by sector, in each of the 24 world regions encompassing the 143 countries examined here.

Annual average total loads in each sector were then divided into inflexible and flexible loads. Flexible loads consisted of cooling loads subject to storage, low-temperature heating loads subject to storage, hydrogen loads, and all other loads subject to demand response (Table S11). Annual average cooling and heating loads were divided not only into flexible cooling and heating loads subject to storage, but also into flexible cooling and heating loads not subject to storage but still subject to demand response, and into inflexible cooling and heating loads (Methods). Such annual average cooling and heating loads were then converted to time-dependent cooling and heating loads using the time-dependent output from GATOR-GCMOM (Methods). All other loads were converted to time-dependent loads as described in Ref. 3.

LOADMATCH was then run for each region with initial generator nameplate capacities (from Ref. 3) and storage characteristics by country estimated to meet annual average WWS loads. If the first simulation did not result in a stable solution, initial inputs into LOADMATCH were adjusted each subsequent simulation until a zero-load-loss solution was found among all 30-s timesteps during 2050. Success typically occurred within 10 simulation attempts. After one successful simulation, the model was run another 4 to 20 simulations, with further adjustments, to find additional lower-cost solutions. Thus, multiple zero-load loss solutions were obtained for each region, but only the lowest-cost solution is presented here.

3. Results

Table S12 provides the final generator nameplate capacities determined from LOADMATCH, and Table S13 provides the ratio of the final to first-guess generator nameplate capacities. Table S14 gives the final simulation-averaged capacity factors in each region. Table S15 provides the final storage peak charge rates, discharge rates, and capacities (assuming the maximum storage times at peak discharge given in Table S16).

Figure S2 shows the full 2050 time series of WWS power

generation versus load plus losses plus changes in storage plus shedding. Supply matched total load (end-use load plus changes in storage plus losses plus shedding) every 30 s for the year in all 24 regions encompassing the 143 countries. Table S17 confirms exact energy conservation numerically. It provides a detailed budget of energy demand, supply, losses, and changes in storage for each region, and for all regions together. For example, it shows that, summed over all 24 world regions, demand plus losses equals 102,646 TWh during the simulation, and this exactly equals supply plus changes of storage. Of that total, 76,041 TWh is given in Table S17 as the end-use demand. Dividing that by 8747.4875 h of simulation gives 8.693 TW of annual-average end-use WWS load, which is the exact total shown in Table 2. The losses quantified in Table S17 include those from shedding, transfers in and out of storage, and transmission/distribution/maintenance. For example, averaged over all grid regions, 17% of all energy produced was shed. Shedding percentages ranged from 1% in Haiti to 35.3% in Israel.

Table 2 and S18 summarize the resulting energy private and social costs. Energy social costs are energy private costs plus health and climate costs due to energy. The WWS private cost per unit energy includes the costs of new electricity and heat generation, short-distance transmission, long-distance transmission, distribution, heat storage, cold storage, electricity storage, and hydrogen production/compression/storage.

WWS energy private costs (costs of energy alone) are assumed to equal WWS energy social costs, since in 2050, WWS generators, storage, and transmission will result in zero pollutant emissions while in use. Also, their manufacture and decommissioning will be free of energy-related emissions. The health and climate costs of zero emissions are zero.

The 2050 all-energy WWS social cost per unit energy, when weighted by generation among all 24 regions, is 8.94 (7.19−11.3) ¢/kWh-all-energy (USD 2013) (Table 2). Individual regional means range from 6.58 ¢/kWh-all-energy (Iceland) to 12.2 ¢/kWh-all-energy (South Korea) (Table 2). The upfront capital cost to transition all 143 countries while keeping the grid stable is ~$72.8 trillion (USD 2013) (Table 2). This is the estimated energy portion of the *Green New Deal* capital cost for the world. It is the capital cost of generation, storage, and transmission/distribution needed to replace all fossil fuels, bioenergy, and nuclear power with WWS for all energy purposes in the 143 countries. More useful, though, are the aggregate annual private and social costs of transitioning all 143 countries to WWS, $6.8 trillion/yr (Table 2). This compares with an aggregate annual 2050 BAU private cost of $17.7 trillion/yr and social cost of $76.1 trillion/yr (Table 2). In other words, WWS reduces annual aggregate private costs by ~62% and social costs by ~91% (Table S18). The main reason for this reduction is the 57.1% lower end-use energy consumption in the WWS case (Table 2).

Footprint is the physical area on the top surface of soil or water needed for each energy device. It does not include areas of underground structures. Spacing is the area between some devices, such as wind turbines, wave devices, and tidal turbines, needed to minimize interference of the wake of one turbine with downwind turbines. Offshore wind turbines, wave devices, and tidal turbines don't take up land. Rooftop solar takes no new land. No new hydropower is added as part of these plans, and geothermal additions are small. Table S20 indicates that, with the installed power densities given in Table S19, WWS requires only about 0.165% of the world's land for the footprint of new utility PV and CSP plants and 0.485% of the world's land for spacing between new onshore wind turbines. Thus, the total land required to transition 143 countries to WWS is 0.65% of the world's land. Much of this is spacing area that can be used for multiple purposes, including putting some of the utility PV on.

This study also estimates the net change in job numbers due to changes in WWS versus BAU generation, transmission, and storage. The estimate accounts for direct jobs, indirect jobs, and induced jobs. Direct jobs are jobs for project development, onsite construction, onsite operation, and onsite maintenance of the electricity generating facility. Indirect jobs are revenue and supply chain jobs. They include jobs associated with construction material and component suppliers; analysts and attorneys who assess project feasibility and negotiate agreements; banks financing the project; all equipment manufacturers; and manufacturers of blades and replacement parts. The number of indirect manufacturing jobs is included in the number of construction jobs. Induced jobs result from the reinvestment and spending of earnings from direct and indirect jobs. They include jobs resulting from increased business at local restaurants, hotels, and retail stores and for childcare providers, for example. Changes in jobs due to changes in energy prices are not included. Energy price changes may trigger changes in factor allocations among capital, energy input, and labor that result in changes in job numbers. Table S21 gives the estimated numbers of construction and operation jobs produced per megawatt of nameplate capacity installed or kilometer of transmission line installed.

Transitioning to 100% WWS is calculated here to create ~27 million more long-term, full-time jobs than lost among the 24 world regions/143 countries. The number of jobs lost was 25,892,000 (Table S28 of Ref. 3) and the gross number of jobs produced was 52,877,000. Net job gains occurred in 21 out of the 24 regions. The exceptions were Canada, Russia, and parts of Africa, where more job losses in the fossil fuel industry occurred than job gains. However, the job numbers here did not account for the change in job numbers due to the manufacture of electric appliances, vehicles, and machines instead of combustion appliance, vehicles, and machines.

Table 1 shows the fraction of the number of hours of a year during which a cold and a low-temperature heat load is needed somewhere in each world region, as determined by GATOR-GCMOM. A cold load occurs during an hour if the ambient temperature in a model grid cell in any country within a region exceeds the reference building temperature, 294.261 K (70 °F), during any 30-s time step during the hour (Methods). A heat load occurs if the temperature drops below the reference temperature.

Table 1 indicates that heating is required all year somewhere in 17 of the 24 regions, and cooling is required all year in 11 of the 24 regions. The regions with the fewest hours of heating needs were Mauritius and Jamaica, followed by Haiti and Cuba. Those with the least cooling needs were Iceland, New Zealand, Canada, South Korea, and Russia. Another way to look at heating and cooling requirements it to examine the ratio of cooling to heating plus cooling. This ratio was lowest in Iceland, New Zealand, Canada, Russia, South Korea, and Japan, respectively, and highest in Mauritius, the Philippines, Jamaica, Southeast Asia, Cuba, and Haiti, respectively.

Fig. 1 and S1 show the time series of total building heat loads, total building cold loads, solar energy production (from rooftop and utility PV and CSP, all combined), and wind energy production (from onshore and offshore wind combined) resulting from the LOADMATCH simulations, for several regions. Results are shown at an hourly time resolution.

Fig. 1 and S1 also show scatterplots of building heat load versus wind power output, cold load versus wind power output, and wind power output versus solar power output. Table 3 provides the R values from such scatterplots for all regions examined as well as R values for two additional sets of scatterplots, those of heat and cold loads versus solar power output.

Table 3 indicates that a strong or very strong positive correlation exists between low-temperature building heat loads and wind

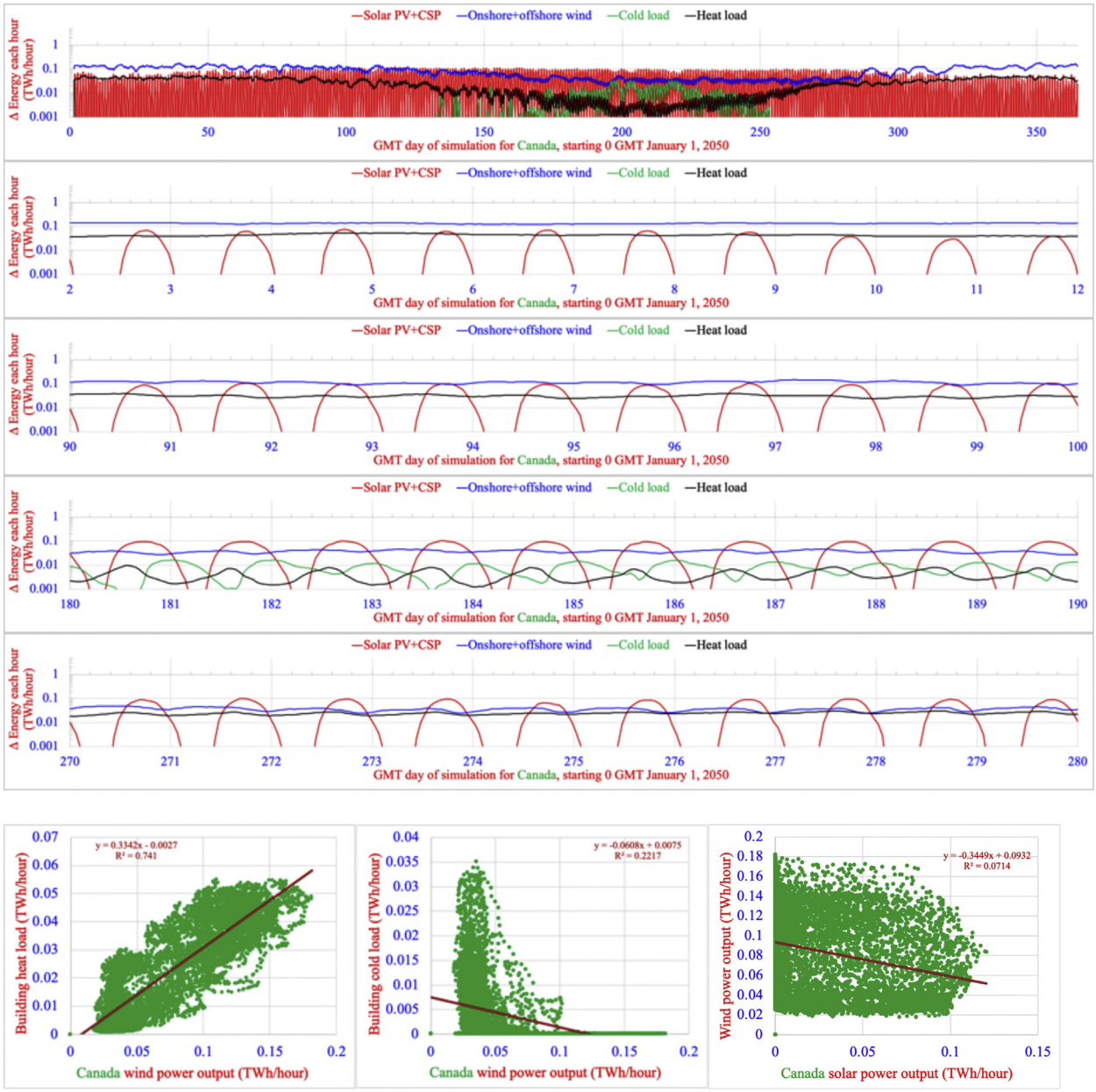

Fig. 1. Modeled time-series of solar PV + CSP electricity production, onshore plus offshore wind energy production, building total cold load, and building total heat load (as used in LOADMATCH), for Canada. The five time-series panels are for the full year (2050) and for 10 days within each season, respectively. Results are shown hourly, so units are energy output (TWh) per hour increment, thus also units of power (TW) averaged over the hour. The last set of panels shows correlation plots of building heat load versus wind power output; building cold load versus wind power output; and wind power output versus solar power output, obtained from all hourly data in the first panel.

power output in 9 of the 24 world regions. A moderate correlation exists in 6 more regions. Heat loads are needed on cool or cold days, so this result indicates that the greater the heat load (the colder the day), the greater the wind energy output.

The regions with the strongest positive correlation are (starting from highest) Canada, Central America, Europe, Taiwan, Russia, Southeast Asia, and the United States. Thus aggregated (over the region) wind energy output is strongly or very strongly correlated with aggregate building heat loads in four of the largest regions of the world with significant heating requirements (Canada, Europe, Russia, and the United States). Moderate correlations were also found in China and Iceland.

Locations with virtually no correlation include Jamaica, Haiti, Mauritius, New Zealand, the Philippines, and South Korea. All of these nations are islands or a peninsula (South Korea), and all are small. All except South Korea and New Zealand are in the Tropics and have a very small heating load relative to cooling load (Table 1). New Zealand lies in the midst of the “Roaring 40’s” westerly wind band but also has a daily sea breeze everywhere and terrain that breaks up some of the wind. Due to its small size (similarly with South Korea), its winds cannot be aggregated over so large of an area as with Canada or Russia, for example, to smoothen its output sufficiently to command a high correlation like the latter countries. In sum, the conclusion found here that wind energy correlates strongly or moderately with building heat load applies primarily to large geographical regions with high heat loads (and some small ones as well, such as Iceland and Taiwan), but does not apply to several small island countries, most of which are in the tropics, but

Table 3
R values from scatterplot of hourly (during the year) GATOR-GCMOM-modeled (a) heat load versus wind energy output; (b) cold load versus wind energy output; (c) heat load versus solar energy output; (d) cold load versus solar energy output; and (e) wind energy output versus solar energy output.

Region	(a) Heat load vs. wind power output	(b) Cold load vs. wind power output	(c) Heat load vs. solar power output	(d) Cold load vs. solar power output	(e) Wind vs. solar power output
Africa	0.38	(0.25)	(0.07_	(0.11)	*(0.45)*
Australia	*0.58*	*(0.50)*	0.04	(0.05)	(0.28)
Canada	**0.86**	*(0.47)*	(0.23)	0.01	(0.27)
Central America	**0.82**	**(0.62)**	0.01	(0.13)	(0.20)
Central Asia	*0.50*	(0.38)	(0.14)	0.15	(0.38)
China	*0.47*	(0.19)	(0.03)	(0.09)	(0.18)
Cuba	0.29	*(0.53)*	0.02	(0.10)	(0.18)
Europe	**0.80**	**(0.60)**	(0.30)	0.16	(0.37)
Haiti	0.17	(0.34)	0.29	(0.18)	(0.15)
Iceland	*0.50*	–	–	–	–
India	*0.43*	(0.20)	0.10	(0.11)	(0.21)
Israel	0.34	(0.21)	(0.20)	0.33	(0.18)
Jamaica	0.14	*(0.42)*	0.01	0.00	(0.07)
Japan	*0.45*	(0.26)	0.08	(0.01)	(0.09)
Mauritius	0.04	*(0.51)*	(0.00)	0.00	(0.15)
Mideast	**0.63**	*(0.52)*	(0.16)	0.23	(0.38)
New Zealand	0.11	(0.06)	(0.04)	(0.05)	(0.17)
Philippines	0.06	(0.39)	*0.56*	*(0.44)*	(0.11)
Russia	**0.76**	*(0.53)*	(0.35)	0.06	(0.36)
South America	**0.60**	**(0.61)**	0.13	(0.19)	(0.07)
Southeast Asia	**0.74**	**(0.64)**	0.23	(0.38)	0.06
South Korea	0.01	(0.02)	(0.01)	(0.08)	(0.09)
Taiwan	**0.78**	*(0.56)*	(0.09)	(0.08)	(0.14)
United States	**0.73**	*(0.56)*	(0.10)	(0.03)	(0.20)

Correlations are very strong for R = 0.8–1; strong for R = 0.6–0.79; moderate for R = 0.4–0.59; weak for 0.2–0.39; and very weak for 0-0.19 [37]. Very strong and strong R values are in bold; moderate values are in italics, and the rest are plain. Parentheses indicate negative correlations. All other correlations are positive.

also New Zealand and South Korea.

Table 3 also indicates that a negative correlation exists in all regions between building cold loads and wind power output. Cold loads are needed on warm or hot days, so this result indicates that the greater the cold load (hotter the day), the lower the wind energy output. This result (winds are weaker on warmer days) is expected for the same reason that winds are stronger on colder days, as discussed shortly. However, the negative correlation between cold loads and wind power is generally weaker than the positive correlation between warm loads and wind power.

Table 3 further shows correlations between building heating and cooling loads and solar power output. None of the correlations in either of these cases is strong or very strong. The correlation in only one location is moderate. Virtually all correlations are weak or very weak. One might expect that on days with high cold loads (warm or hot days), solar output would be high (thus a positive correlation between building cold loads and solar power output). This does occur in several regions, but the correlation is negative in others. One reason for the weak correlations is that the air is cold during the day in many locations despite the presence of sunlight. For example, Table 1 indicates that cold loads dominate in only 10 of 24 world regions. In most regions, warm loads dominate, even during the day, because the regions are at high latitude or have some places at high altitude. A second reason is that, when cold loads occur on sunny days, the air remains warm and cold loads persist during the night. In those cases, cold loads are correlated with both high solar output and low solar output, weakening the overall correlation.

Table 1 lastly shows the correlation between wind and solar output. The correlation is remarkably consistently negative in all except one region (Southeast Asia), where it is positive but very weak. The negative correlations are mostly weak but are moderate in a couple locations. The reason for this anticorrelation is simply that winds are generally strong within low-pressure systems, which are also characterized by low temperatures, strong pressure gradients, and heavy cloud cover, thus low solar output. Solar output is much greater within high pressure systems, which are characterized by cloud-free skies, warm weather, and weak pressure gradients (thus weak winds). As such, wind and solar are complementary in nature. When the wind is not blowing during the day, the sun is often shining and vice versa. The implication of this is that, where possible, wind and solar energy should be both be built to reduce the variability of either one alone, thus to smoothen out the power supply.

4. Discussion and conclusions

The high-resolution time series plots in Fig. 1 and S1 indicate that modeled heat loads peak after sunrise and are minimum before sunset, as expected (since the coldest time of day generally occurs when incoming solar radiation first equals outgoing thermal-infrared radiation, which occurs after sunrise; the warmest time of day occurs when incoming solar decreases until it equals outgoing thermal-infrared, and that occurs before sunset). In addition, Fig. 1 and S1 indicate that wind energy output, which is dominated by wind turbines over land in most regions in this study (Table S12), peaks primarily at night and decreases only after the peak heating load decreases.

The modeled wind turbine hub height in GATOR-GCMOM is 100 m, and the rotor diameter is 126 m. Thus, wind energy output depends on wind speeds between 37 m and 163 m above the ground. The model accounts for wind speeds in multiple layers between a turbine blade's lowest (37 m) and highest (163 m) extents when determining output [35]. Excess wind (or solar) electricity beyond the load needed is put into electricity storage, heat storage, cold storage, and hydrogen storage. If all storage is full, excess electricity is shed.

Wind energy output in the model and in the real world often

peak at night over land because colder ground temperatures at night reduce convective turbulence, stabilizing the air. Stabilizing the air by any mechanism reduces the downward transfer of horizontal momentum [38]. Thus, at night fast winds aloft (37–163 m) are not mixed with slow surface winds as they are during the day, increasing wind speeds aloft at night relative to the day. Only after convection strengthens during the day, around noon, do daytime wind speeds aloft decline due to the turbulent mixing of slow winds from the surface to aloft.

In some locations (e.g., Europe, Figure S1), wind energy output follows heat load remarkably well on a diurnal basis. This is not only due to the day versus night wind speed peaks just discussed, but also due to the fact that low temperatures, which create heat loads, often occur behind cold fronts, where pressure gradients are strong, thus winds are fast [39]. Low temperatures over land also often occur in the presence of strong temperature gradients, which produce strong pressure gradients and strong winds [39].

In sum, a physical basis appears to explain why wind energy output is strongly positively correlated with building heat loads in large, cold regions. Such a correlation is helpful for matching all-energy power demand with clean, renewable WWS supply in such regions. Low-cost solutions to the grid reliability problem were found here in such regions (e.g., in Canada – all energy is 8.24 ¢/kWh; Europe, 8.30 ¢/kWh; Russia, 8.20 ¢/kWh; United States, 9.20 ¢/kWh – Table 2). Some regions with a high correlation have slightly higher costs (e.g., Taiwan, 10.8 ¢/kWh) because their limited land area requires them to rely on more expensive offshore wind. On the other hand, lower-cost solutions are available in some regions without a correlation (e.g., New Zealand, 8.33 ¢/kWh) due to the abundance of inexpensive WWS resources in such regions.

A significant policy implication of this study is that wind energy can help meet peaks in building heat demand during harsh winter storms. To be helpful, though, wind turbines used for such applications should contain de-icing equipment. A case in point is the freezing, winter storm that cut across Texas during February 14–18, 2021. The low temperatures caused equipment failures for natural gas, coal, nuclear, and wind electricity generation, with natural gas being the largest source of electricity and failure. A number of frozen wind turbines had to be shut because none had de-icing equipment. The remaining turbines, however, produced more electricity than was normally expected due to high winds during the storm. This result implies that more, rather than fewer, turbines, but all with de-icing equipment, would help meet heating loads during a severe winter storm. In sum, this work should help to inspire wind-related solutions to meeting building heating loads in cold regions on Earth.

A final implication is that, because wind and solar output are negatively correlated, they are complementary in nature, and building both in the same region helps to create a less variable energy supply than if only one or the other alone is built.

Author contributions

Conceptualization, Methodology, Investigation, Software, Writing, Review, Visualization: M.Z.J.

Declaration of competing interest

There are no conflicts of interest to declare.

Acknowledgments

This research did not receive any funding from any source. The data from this paper, including data going into all plots, and the LOADMATCH model, are available upon request from jacobson@stanford.edu.

Appendix A. Supplementary data

Supplementary data to this article can be found online at https://doi.org/10.1016/j.segy.2021.100009.

References

[1] Jacobson MZ, Delucchi MA. A Path to Sustainable Energy by 2030. Scientific American *November*; 2009.
[2] Jacobson MZ, Delucchi MA, Bauer ZAF, Goodman SC, Chapman WE, Cameron MA, , C. Alphabetical: Bozonnat, Chobadi L, Clonts HA, Enevoldsen P, Erwin JR, Fobi SN, Goldstrom OK, Hennessy EM, Liu J, Lo J, Meyer CB, Morris SB, Moy KR, O'Neill PL, Petkov I, Redfern S, Schucker R, Sontag MA, Wang J, Weiner E, Yachanin AS. 100% clean and renewable wind, water, and sunlight (WWS) all-sector energy roadmaps for 139 countries of the world. Joule 2017;1:108–21.
[3] Jacobson MZ, Delucchi MA, Cameron MA, Coughlin SJ, Hay C, Manogaran IP, Shu Y, von Krauland A-K. Impacts of Green New Deal energy plans on grid stability, costs, jobs, health, and climate in 143 countries. One Earth 2019;1:449–63.
[4] Jacobson MZ, Delucchi MA, Cameron MA, Mathiesen BV. Matching demand with supply at low cost among 139 countries within 20 world regions with 100 percent intermittent wind, water, and sunlight (WWS) for all purposes. Renew. Energy 2018;123:236–48.
[5] Bogdanov D, Farfan J, Sadovskaia K, Aghahosseini A, Child M, Gulagi A, Oyewo AS, Barbosa LSNS, Breyer C. Radical transformation pathway towards sustainable electricity via evolutionary steps. Nat. Commun. 2019;10:1077.
[6] Mason IG, Page SC, Williamson AG. A 100% renewable energy generation system for New Zealand utilizing hydro, wind, geothermal, and biomass resources. Energy Pol. 2010;38:3973–84.
[7] Hart EK, Jacobson MZ. A Monte Carlo approach to generator portfolio planning and carbon emissions assessments of systems with large penetrations of variable renewables. Renew. Energy 2011;23:2278–86.
[8] Budischak C, Sewell D, Thompson H, Mach L, Veron DE, Kempton W. Cost-minimized combinations of wind power, solar power, and electrochemical storage, powering the grid up to 99.9% of the time. J. Power Sources 2013;225:60–74.
[9] Elliston B, MacGill I, Diesendorf M. Comparing least cost scenarios for 100% renewable electricity with low emission fossil fuel scenarios in the Australian National Electricity Market. Renew. Energy 2014;66:196–204.
[10] Becker S, Frew BA, Andresen GB, Zeyer T, Schramm S, Greiner M, Jacobson MZ. Features of a fully renewable U.S. electricity system: optimized mixes of wind and solar PV and transmission grid extensions. Energy 2014;72:443–58.
[11] Blakers A, Lu B, Socks M. 100% renewable electricity in Australia. Energy 2017;133:417–82.
[12] Zapata S, Casteneda M, Jiminez M, Aristizabel AJ, Franco CJ, Dyner I. Long-term effects of 100% renewable generation on the Colombian power market. Sustainable Energy Technologies and Assessments 2018;30:183–91.
[13] Esteban M, Portugal-Pereira J, Mclellan BC, Bricker J, Farzaneh H, Djalikova N, Ishihara KN, Takagi H, Roeber V. 100% renewable energy system in Japan: smoothening and ancillary services. Appl. Energy 2018;224:698–707.
[14] Sadiqa A, Gulagi A, Breyer C. Energy transition roadmap towards 100% renewable energy and role of storage technologies for Pakistan by 2050. Energy 2018;147:518–33.
[15] Liu H, Andresen GB, Greiner M. Cost-optimal design of a simplified highly renewable Chinese network. Energy 2018;147:534–46.
[16] Lund H, Mathiesen BV. Energy system analysis of 100% renewable energy systems-The case of Denmark in years 2030 and 2050. Energy 2009;34:524–31.
[17] Mathiesen BV, Lund H, Karlsson K. 100% renewable energy systems, climate mitigation, and economic growth. Appl. Energy 2011;88:488–501.
[18] Connolly D, Mathiesen BV. Technical and economic analysis of one potential pathway to a 100% renewable energy system. Intl. J. Sustainable Energy Planning & Management 2014;1:7–28.
[19] Jacobson MZ, Delucchi MA, Cameron MA, Frew BA. A low-cost solution to the grid reliability problem with 100% penetration of intermittent wind, water, and solar for all purposes. Proc. Natl. Acad. Sci. Unit. States Am. 2015;112(15):60–5.
[20] Mathiesen BV, Lund H, Connolly D, Wenzel H, Ostergaard PZ, Moller B, Nielsen S, Ridjan I, Karnoe P, Sperling K, Hvelplund FK. Smart energy systems for coherent 100% renewable energy and transport solutions. Appl. Energy 2015;145:139–54.
[21] Bogdanov D, Toktarova A, Breyer C. Transition towards 100% renewable power and heat supply for energy intensive economics and severe continental climate conditions: case for Kazakhstan. Appl. Energy 2019;253:113606.
[22] Hansen K, Mathiesen BV, Skov IR. Full energy system transition towards 100% renewable energy in Germany in 2050. Renew. Sustain. Energy Rev. 2019;102:1–13.
[23] Steinke F, Wolfrum P, Hoffmann C. Grid vs. storage in a 100% renewable Europe. Renew. Energy 2013;50:826–32.

[24] Zozmann E, Goke L, Kendziorski M, del Angel CR, von Hirschhausen C, Winkler J. 100% renewable energy scenarios for North America-Spatial distribution and network constraints. Energies 2021;14:658.
[25] Connolly D, Lund H, Mathiesen BV. Smart energy Europe: the technical and economic impact of one potential 100% renewable energy scenario for the European Union. Renew. Sustain. Energy Rev. 2016;60:1634–53.
[26] Aghahosseini A, Bogdanov D, Barbosa LSNS, Breyer C. Analyzing the feasibility of powering the Americas with renewable energy and inter-regional grid interconnections by 2030. Renew. Sustain. Energy Rev. 2019;105:187–205.
[27] Lund H, Andersen AN, Ostergaard PA, Mathiesen BV, Connolly D. From electricity smart grids to smart energy systems-A market operation based approach and understanding. Energy 2012;42:96–102.
[28] Connolly D, Lund H, Mathiesen BV, Werner S, Moller B, Persson U, Boermans T, Trier D, Ostergaard PA, Nielsen S. Heat roadmap Europe: combining district heating with heat savings to decarbonise the EU energy system. Energy Pol. 2014;65:475–89.
[29] Drysdale D, Mathiesen BV, Paardekooper S. Transitioning to a 10)% renewable energy system in Denmark by 2050: assessing the impact from expanding the building stock at the same time. Energy Efficiency 2019;12:37–55.
[30] Olsen DJ, Matson N, Sohn MD, Rose C, Dudley J, Goli S, Kiliccote S, et al. Grid Integration of Aggregated Demand Response, Part 1: Load Availability Profiles and Constraints for the Western Interconnection. Berkeley, California: Lawrence Berkeley National Laboratory; 2013. Technical Report LBNL-6417E.
[31] Hale E, Horsey H, Johnson B, Muratori M, Wilson E, et al. The Demand-Side Grid (Dsgrid) Model Documentation. Golden, CO: National Renewable Energy Laboratory; 2018. NREL/TP-6A20-71492, https://www.nrel.gov/docs/fy18osti/71492.pdf.
[32] Toktarova A, Gruber L, Hlusiak M, Bogdanov D, Breyer C. Long term load projection in high resolution for all countries globally. Int. J. Electr. Power Energy Syst. 2019;111:160–81.
[33] Jacobson MZ. GATOR-GCMOM: a global through urban scale air pollution and weather forecast model: 1. Model design and treatment of subgrid soil, vegetation, roads, rooftops, water, sea ice, and snow. J. Geophys. Res.: Atmosphere 2001;106:5385–401.
[34] Jacobson MZ, Kaufmann YJ, Rudich Y. Examining feedbacks of aerosols to urban climate with a model that treats 3-D clouds with aerosol inclusions. J. Geophys. Res.: Atmosphere 2007;112:D24205.
[35] Jacobson MZ, Archer CL. Saturation wind power potential and its implications for wind energy. Proc. Natl. Acad. Sci. Unit. States Am. 2012;109(15):679–84.
[36] Jacobson MZ, Jadhav V. World estimates of PV optimal tilt angles and ratios of sunlight incident upon tilted and tracked PV panels relative to horizontal panels. Sol. Energy 2018;169:55–66.
[37] Evans JD. Straightforward Statistics for the Behavioral Sciences. Pacific Grove, CA: Brooks/Cole Publishing; 1996.
[38] Jacobson MZ, Kaufmann YJ(. Wind reduction by aerosol particles. Geophys. Res. Lett. 2006;33:L24814. https://doi.org/10.1029/2006GL027838.
[39] Wind Logger. How does cold weather affect wind speed?. https://www.windlogger.com/blogs/news/how-does-cold-weather-affect-wind-speed; 2020. accessed July 17, 2020.

Electronic Supplementary Information

On the Correlation Between Building Heat Demand and Wind Energy Supply and How it Helps to Avoid Blackouts

Mark Z. Jacobson

This supplementary information file contains additional tables and figures to help explain more fully the methods and results found in this study.

Supporting Tables

Table S1. Estimated average building-component surface areas (taken as an average U.S. residential unit), U-values, and products of the surface area and U-value assumed for the simulations here.

Building component	Surface area (A, m^2)	U-value (U, W/m^2-K)	$A \times U$ (W/K)
Floor	223	0.22	49.1
Roof	223	0.18	40.1
Windows	45.5	1.4	63.7
Walls	136.5	0.28	38.2
Overall	628	0.304	191

For buildings with high U-values (high heat losses or gains), a greater heating or cooling load is needed than for buildings with low U-values in order to maintain a constant indoor temperature.

Table S2. Several of the processes treated in the LOADMATCH model.

Parameter	Is the process treated?
Onshore and offshore wind electricity	Yes
Residential, commercial/government rooftop PV electricity	Yes
Utility PV electricity	Yes
CSP electricity	Yes
Geothermal electricity	Yes
Tidal and wave electricity	Yes
Direct solar and geothermal heat	Yes
Battery storage	Yes
CSP storage	Yes
Pumped hydropower storage	Yes
Existing hydropower dam storage	Yes
Added hydropower turbines	No
Heat storage (water tanks, underground)	Yes
Cold storage (water tanks, ice)	Yes
Hydrogen storage in tanks	Yes
Hydrogen fuel cell vehicles for long-distance, heavy transport	Yes
Battery-electric vehicles for all other transport	Yes
District heating	Yes
Electric heat pumps for building cooling and air/water heating	Yes
Electric furnaces and heat pumps for industrial heat	Yes
Wind, PV, CSP, solar heat, wave supply calculated in GATOR-GCMOM	Yes
Building heat and cold loads calculated in GATOR-GCMOM	Yes
Array losses due to wind turbines competing for kinetic energy	Yes
Losses from T&D, storage, shedding, downtime	Yes
Perfect transmission interconnections	Yes
Costs of all generation, all storage, short- and long-distance T&D	Yes
Avoided cost of air pollution damage	Yes
Avoided cost of climate damage	Yes
Land footprint and spacing requirements	Yes
Changes in job numbers	Yes

Table S3. Fraction of 2010 annual average residential or commercial total energy (electricity plus heat) load that is heat load (the rest is electricity load), before and after converting the heat load to electricity load for heat pumps (with a coefficient of performance of CP=4), by country or region. Heat load includes load for both air and water heating. Data in Column (A) are from Ref. S2, who derived it from data in Ref. S3.

Country or region	(A) Fraction of total load in the residential or commercial sector that is low-temperature heat load	(B) Fraction of total load in the residential or commercial sector that is low-temperature heat load produced by electricity with heat pumps = (A/CP)/((A/CP)+1-A) (F_h)
Asia other	0.816	0.526
Australia	0.649	0.316
Brazil	0.660	0.327
Canada	0.723	0.395
China	0.857	0.600
Russia	0.881	0.649
France	0.757	0.438
Germany	0.804	0.506
India	0.856	0.598
Italy	0.816	0.526
Japan	0.665	0.332
LAM other	0.756	0.436
MEA other	0.743	0.420
Nigeria	0.963	0.867
OECD other	0.748	0.426
Poland	0.865	0.616
RE other	0.811	0.518
South Africa	0.746	0.423
United Kingdom	0.805	0.508
United States	0.689	0.356
World average	0.787	0.480

Asia other = Asia other than China and India; LAM other = Latin America other than Brazil; MEA other = Middle East and Africa other than South Africa and Nigeria; OECD other = countries in the Organization for Economic Cooperation and Development other than Australia, France, Germany, Japan, Italy, United Kingdom, United States; RE other = reforming economies in Eastern Europe and the former Soviet Union other than Poland and Russia.

Table S4. Parameters for estimating thermal energy demand in different world regions. These parameters are used in the Equations in Notes S29-S31 of Ref. S1. F_{dh} is the fraction of the 2050 combined air heating, water heating, air conditioning, and refrigeration demand that is subject to district heating, thus subject to thermal energy storage. F_{H2} is the fraction of total 2050 all-sector end-use demand needed to produce, compress, and store hydrogen for transportation. The average across all regions is 6.01%, which represents 37.1% of the transportation load. The remaining values are the fractions of either residential, commercial, or industrial 2050 annual average load (given in Table S10) that is for air heating (F_{ah}), water heating (F_{wh}), air cooling (F_{ac}), refrigeration (F_{rf}), or high-temperature industrial processes (F_{ht}).

			Residential			Commercial				Industrial			
Region	F_{dh}	F_{H2}	F_{ah}	F_{wh}	F_{ac}	F_{ah}	F_{wh}	F_{ac}	F_{rf}	F_{ht}	F_{ah}	F_{ac}	F_{rf}
Africa	0.1	0.084	0.37	0.16	0.38	0.38	0.08	0.43	0.32	0.66	0.015	0.048	0.024
Australia	0.1	0.073	0.22	0.09	0.04	0.26	0.06	0.05	0.04	0.62	0.052	0.010	0.024
Canada	0.2	0.056	0.28	0.12	0.01	0.33	0.07	0.01	0.01	0.64	0.061	0.002	0.024
Central America	0.1	0.102	0.31	0.13	0.18	0.36	0.08	0.21	0.16	0.62	0.039	0.023	0.024
Central Asia	0.01	0.050	0.37	0.16	0.38	0.43	0.09	0.38	0.28	0.64	0.028	0.034	0.024
China	0.3	0.031	0.42	0.18	0.09	0.49	0.10	0.11	0.08	0.64	0.052	0.011	0.024
Cuba	0.15	0.035	0.31	0.13	0.45	0.36	0.08	0.45	0.33	0.62	0.007	0.055	0.024
Europe	0.5	0.067	0.33	0.14	0.02	0.39	0.08	0.02	0.02	0.59	0.059	0.004	0.024
Haiti	0.2	0.095	0.31	0.13	0.45	0.36	0.08	0.45	0.33	0.62	0.009	0.053	0.024
Iceland	0.92	0.033	0.30	0.13	0.00	0.35	0.07	0.00	0.00	0.59	0.062	0.000	0.024
India	0.1	0.049	0.42	0.18	0.32	0.49	0.10	0.32	0.24	0.71	0.009	0.053	0.024
Israel	0.2	0.079	0.22	0.09	0.06	0.26	0.06	0.07	0.05	0.62	0.049	0.013	0.024
Jamaica	0	0.105	0.31	0.13	0.45	0.36	0.08	0.45	0.33	0.62	0.001	0.062	0.024
Japan	0.1	0.054	0.23	0.10	0.01	0.27	0.06	0.01	0.01	0.59	0.060	0.003	0.024
Mauritius	0.2	0.187	0.29	0.13	0.46	0.35	0.07	0.46	0.34	0.71	0.001	0.062	0.024
Middle East	0.05	0.069	0.29	0.13	0.17	0.35	0.07	0.20	0.15	0.71	0.040	0.023	0.024
New Zealand	0.05	0.064	0.22	0.09	0.00	0.26	0.06	0.00	0.00	0.62	0.062	0.000	0.024
Philippines	0.05	0.102	0.37	0.16	0.38	0.43	0.09	0.38	0.28	0.64	0.001	0.062	0.024
Russia	0.5	0.051	0.46	0.19	0.02	0.54	0.11	0.02	0.01	0.72	0.060	0.002	0.024
South America	0.1	0.073	0.27	0.12	0.37	0.31	0.07	0.43	0.31	0.64	0.026	0.036	0.024
Southeast Asia	0.1	0.099	0.37	0.16	0.38	0.43	0.09	0.38	0.28	0.64	0.007	0.055	0.024
South Korea	0.15	0.054	0.30	0.13	0.01	0.35	0.07	0.02	0.01	0.59	0.060	0.003	0.024
Taiwan	0.15	0.059	0.37	0.16	0.23	0.43	0.09	0.27	0.20	0.64	0.039	0.024	0.024
United States	0.2	0.083	0.25	0.11	0.04	0.29	0.06	0.05	0.04	0.64	0.054	0.009	0.024

Table S5. The 24 world regions comprised of 143 countries treated in this study.

Region	Country(ies) Within Each Region
Africa	Algeria, Angola, Benin, Botswana, Cameroon, Congo, Democratic Republic of the Congo, Egypt, Eritrea, Ethiopia, Gabon, Ghana, Ivory Coast, Kenya, Libya, Morocco, Mozambique, Namibia, Niger, Nigeria, Senegal, South Africa, South Sudan, Sudan, Tanzania, Togo, Tunisia, Zambia, Zimbabwe
Australia	Australia
Canada	Canada
Central America	Costa Rica, El Salvador, Guatemala, Honduras, Mexico, Nicaragua, Panama
Central Asia	Kazakhstan, Kyrgyz Republic, Pakistan, Tajikistan, Turkmenistan, Uzbekistan
China	China, Hong Kong, Democratic Republic of Korea, Mongolia
Cuba	Cuba
Europe	Albania, Austria, Belarus, Belgium, Bosnia-Herzegovina, Bulgaria, Croatia, Cyprus, Czech Republic, Denmark, Estonia, Finland, France, Germany, Gibraltar, Greece, Hungary, Ireland, Italy, Kosovo, Latvia, Lithuania, Luxembourg, Macedonia, Malta, Moldova Republic, Montenegro, Netherlands, Norway, Poland, Portugal, Romania, Serbia, Slovakia, Slovenia, Spain, Sweden, Switzerland, Ukraine, United Kingdom
Haiti	Haiti, Dominican Republic
Iceland	Iceland
India	India, Nepal, Sri Lanka
Israel	Israel
Jamaica	Jamaica
Japan	Japan
Mauritius	Mauritius
Mideast	Armenia, Azerbaijan, Bahrain, Iran, Iraq, Jordan, Kuwait, Lebanon, Oman, Qatar, Saudi Arabia, Syrian Arab Republic, Turkey, United Arab Emirates, Yemen
New Zealand	New Zealand
Philippines	Philippines
Russia	Georgia, Russia
South America	Argentina, Bolivia, Brazil, Chile, Colombia, Curacao, Ecuador, Paraguay, Peru, Suriname, Trinidad and Tobago, Uruguay, Venezuela
Southeast Asia	Bangladesh, Brunei Darussalam, Cambodia, Indonesia, Malaysia, Myanmar, Singapore, Thailand, Vietnam
South Korea	South Korea
Taiwan	Taiwan
United States	United States

Table S6. Present value of the mean 2019 to 2050 lifecycle costs of new storage capacity and round-trip efficiencies of the storage technologies treated here.

Storage technology	Present-value of lifecycle cost of new storage ($/kWh-max energy storage capacity)			Round-trip charge/store/ discharge efficiency (percent)
	Middle	Low	High	
Electricity				
PHS	14	12	16	80
CSP-PCM	20	15	23	99
LI Batteries	60	30	90	85
Cold				
CW-STES	6.5	0.13	12.9	84.7
ICE	36.7	12.9	64.5	82.5
Heat				
HW-STES	6.5	0.13	12.9	83
UTES	0.90	0.071	1.71	56

From Ref. S1.

PHS = pumped hydropower storage; CSP-PCM = concentrated solar power with phase change material for storage; LI Batteries = lithium ion batteries; CW-STES = cold water sensible-heat thermal energy storage; ICE = ice storage; HW-STES = hot water sensible-heat thermal energy storage; UTES = underground thermal energy storage (modeled as borehole). PHS efficiency is the ratio of electricity delivered to the sum of electricity delivered and electricity used to pump the water.

Storage costs per unit energy generated in the overall system of each storage technology are calculated as the product of the maximum energy storage capacity (Table S15) and the lifecycle-averaged capital cost of storage per unit maximum energy storage capacity (this table), annualized with the same discount rate as for power generators (Table S7, footnote), but with 2050 storage lifetimes of 17 (12 to 22) years for batteries and 32.5 (25 to 40) years all other storage, all divided by the annual average end-use load met.

The CSP-PCM cost is for the PCM material and storage tanks. The CSP-PCM efficiency is the ratio of the heat available for the steam turbine after storage to the heat from the solar collector that goes into storage. The additional energy losses due to reflection and absorption by the CSP mirrors (45% of incident solar energy is lost to reflection) and due to converting CSP heat to electricity (71.3% of heat is wasted and only 28.7% is converted to electricity) are accounted for in the CSP efficiency without storage. Battery efficiency is the ratio of electricity delivered to electricity put into the battery. CW-STES and HW-STES efficiencies are the ratios of the energy returned as cooling and heating, respectively, after storage, to the electricity input into storage. The UTES efficiency is the fraction of heated fluid entering underground storage that is ultimately returned during the year (either short or long term) as air or water heat for a building.

Table S7. Parameters for determining costs of energy from electricity and heat generators.

	Capital cost new installations ($Million/MW)	O&M Cost ($/kW/yr)	Decom-missioning cost (% of capital cost)	Lifetime (years)	TDM losses (% of energy generated)
Onshore wind	1.27 (1.07-1.47)	37.5 (35-40)	1.25 (1.2-1.3)	30 (25-35)	7.5 (5-10)
Offshore wind	1.86 (1.49-2.24)	80 (60-100)	2 (2-2)	30 (25-35)	7.5 (5-10)
Residential PV	2.97 (2.65-3.28)	27.5 (25-30)	0.75 (0.5-1)	44 (41-47)	1.5 (1-2)
Commercial/government PV	2.06 (1.80-2.31)	16.5 (13-20)	0.75 (0.5-1)	46 (43-49)	1.5 (1-2)
Utility-scale PV	1.32 (1.16-1.49)	19.5 (16.5-22.5)	0.75 (0.5-1)	48.5 (45-52)	7.5 (5-10)
CSP with storage[a]	4.84 (4.42-5.26)	50 (40-60)	1.25 (1-1.5)	45 (40-50)	7.5 (5-10)
Geothermal for electricity	3.83 (2.47-5.18)	45 (36-54)	2.5 (2-3)	45 (40-50)	7.5 (5-10)
Hydropower	2.81 (2.38-3.25)	15.5 (15-16)	2.5 (2-3)	85 (70-100)	7.5 (5-10)
Wave	4.01 (2.74-5.28)	175 (100-250)	2 (2-2)	45 (40-50)	7.5 (5-10)
Tidal	3.57 (2.85-4.29)	125 (50-200)	2.5 (2-3)	45 (40-50)	7.5 (5-10)
Solar thermal for heat	1.22 (1.12-1.33)	50 (40-60)	1.25 (1-1.5)	35 (30-40)	3 (2-4)
Geothermal for heat	3.83 (2.47-5.18)	45 (36-54)	2 (1-3)	45 (40-50)	7.5 (5-10)

From Ref. S1.

Capital costs (per MW of nameplate capacity) are an average of 2019 and 2050. O&M=Operation and maintenance. TDM = transmission/distribution/maintenance. TDM losses are a percentage of all energy produced by the generator and are an average over short and long-distance (high-voltage direct current) lines.

Short-distance transmission costs are $0.0105 (0.01-0.011)/kWh. Distribution costs are $0.02375 (0.023-0.0245)/kWh. Long-distance transmission costs are $0.00406 (0.00152-0.00903)/kWh (in USD 2013) (Ref. S1) which assumes 1,200 to 2,000 km lines. It is assumed that 30% of all annually-averaged electricity generated is subject to long-distance transmission in all regions except Cuba, Haiti, Iceland, Israel, Jamaica, Mauritius, South Korea, and Taiwan (0%); New Zealand (15%); and Central America, Japan, and the Philippines (20%).

The discount rate used for generation, storage, transmission/distribution, and social costs is a social discount rate of 2 (1-3)%.

[a]The capital cost of CSP with storage includes the cost of extra mirrors and land but excludes costs of phase-change material and storage tanks, which are given in Table S6. The cost of CSP with storage depends on the ratio of the CSP storage maximum charge rate plus direct electricity use rate (which equals the maximum discharge rate) to the CSP maximum discharge rate. For the purpose of benchmarking the "CSP with storage" cost in this table, we use a ratio of 3.2:1. (In other words, if 3.2 units of sunlight come in, a maximum of 2.2 units can go to storage and a maximum of 1 unit can be discharged directly as electricity at the same time.) The ratio for "CSP no storage" is 1:1. In our actual simulations and cost calculations, we assume a ratio of 2.61:1 for CSP with storage[1] and find the cost for this assumed ratio by interpolating between the "CSP with storage" benchmark value and the "CSP no storage" value in this table.

Table S8. Parameters in the calculation of the value of statistical life over time and by country.

Parameter	LCHB	Middle	HCLB
U.S. VOSL in base year 2006 ($VOSL_{US,BYV}$) ($mil/death USD 2006)	9.00	7.00	5.00
U.S. VOSL in target year 2050 ($VOSL_{US,Y}$) ($mil/death USD 2013)	15.37	10.40	6.47
2006 global average VOSL ($mil/death USD 2006)	4.00	3.48	3.43
2050 global average VOSL ($mil/death USD 2013)	8.15	7.09	6.99
U.S. GDP per capita in 2006 ($G_{US,BYV}$) (USD $/person 2006)	52,275	52,275	52,275
U.S. GDP per capita target year 2050 ($G_{US,Y}$) (USD $/person 2013)	96,093	96,093	96,093
Multiplier for morbidity impacts (F_1)	1.25	1.15	1.05
Multiplier for non-health impacts (F_2)	1.10	1.10	1.05
Fractional reduction in mortalities per year (ΔA_c)	-0.014	-0.015	-0.016
Exponent giving change in mortality with population change (κ)	1.14	1.11	1.08
Fraction of country's VOSL fixed at U.S. TY value (T)	0.10	0.00	0.00
GDP/capita elasticity ($\gamma_{GDP,US,BYV}$) of VOSL, U.S. base year 2006	0.75	0.50	0.25
GDP/capita elasticity (γ_{GDP}) of VOSL, all years	-0.15	-0.15	-0.15

These parameters, from Ref. S1, are applied to the equations in Note S39 of Ref. S1. LCHB = low cost, high benefit. HCLB = high cost, low benefit. VOSL = value of statistical life. GDP = gross domestic product at purchasing power parity (PPP). Multiply LCHB VOSL by the high estimate of air pollution premature deaths to obtain the high estimate of air pollution cost in the BAU case (or greatest avoided air pollution benefit in the WWS case).

Table S9. Low, mid, and high estimates of the social cost of carbon (SCC).

Parameter	Low estimate	Mid estimate	High estimate
2010 Global SCC (2007 USD)	125	250	600
Annual percentage increase in SCC	1.8	1.5	1.2
2050 Global SCC (2013 USD)	282	500	1,063

Units of the SCC are USD per metric tonne-CO_2e. These parameters are derived from the sources discussed in Note S40 of Ref. S1.

Table S10. 2050 annual average end-use electric plus heat load (GW) by energy sector and region after energy in all sectors has either been electrified or remains as direct low-temperature heat, with the electricity and heat both provided by WWS. Instantaneous loads can be higher or lower than annual average loads. From Ref. S1.

Region	Total	Resi-dential	Com-mercial	Trans-port	Industrial	Agricul-ture/fores-try/fishing	Military/ other
Africa	482	139	33.4	96.9	198	7.57	6.98
Australia	93.6	12.0	18.2	17.2	45.2	1.00	0.00
Canada	152	26.2	27.6	26.9	66.7	3.04	1.25
Central America	154	24.7	12.1	36.9	72.7	3.15	4.85
Central Asia	151	33.78	11.3	18.7	79.4	4.45	3.49
China	2,328	364	122	252	1,489	25.9	74.3
Cuba	8.06	1.67	0.55	0.78	4.71	0.10	0.27
Europe	940	207	178	187	354	12.6	1.19
Haiti	7.54	1.78	0.70	1.68	3.23	0.15	0.00
Iceland	2.98	0.28	0.38	0.29	1.92	0.11	0.01
India	945	160	40.5	117	559	45.9	23.0
Israel	12.8	3.14	2.81	2.34	3.86	0.26	0.41
Jamaica	2.27	0.20	0.05	0.57	1.39	0.07	0.00
Japan	178	30.8	41.4	28.7	75.8	1.08	0.22
Mauritius	1.79	0.26	0.26	0.77	0.49	0.01	0.01
Mideast	678	121	62.2	109	366	11.0	8.18
New Zealand	17.6	2.21	2.68	2.63	9.43	0.61	0.02
Philippines	40.5	7.20	6.25	9.83	16.6	0.56	0.00
Russia	236	59.7	30.6	37.0	106	3.04	0.21
South America	489	62.5	43.5	94.0	274	11.2	3.79
Southeast Asia	583	87.6	52.1	140	296	4.80	3.18
South Korea	155	13.4	33.4	20.2	85.4	2.54	0.28
Taiwan	94.9	11.4	8.15	14.0	57.1	0.68	3.52
United States	939	170	188	194	357	9.62	20.9
Total 2050	8,693	1,542	917	1,408	4,521	149	156

Table S11. Annual average WWS all-sector inflexible and flexible loads (GW) for 2050 by world region. "Total load" is the sum of "inflexible load" and "flexible load." "Flexible load" is the sum of "cold load subject to storage," "low-temperature heat load subject to storage," "load for H_2" production, compression, and storage (accounting for leaks as well), and "all other loads subject to demand response (DR)." Annual average loads are distributed in time as described in the text. Thus, instantaneous loads, either flexible or inflexible, can be much higher or lower than annual average loads. Also shown is the annual hydrogen mass needed in each region, estimated as the load multiplied by 8,760 hr/yr and divided by 59.01 kWh/kg-H_2.

Region	Total end-use load (GW)	Inflex-ible load (GW)	Flex-ible load (GW)	Cold load subject to storage (GW)	Low-temp-erature heat load subject to storage (GW)	Load for H_2 (GW)	All other loads sub-ject to DR	H_2 needed (Tg-H_2/yr)
Africa	482	232	250	9.17	30.2	40.6	170	6.02
Australia	93.6	48.9	44.7	0.38	3.01	6.84	34.5	1.01
Canada	152	77.6	74.0	0.48	8.79	8.54	56.2	1.27
Central America	154	71.6	82.9	1.24	5.42	15.7	60.5	2.33
Central Asia	151	79.3	71.9	0.25	6.23	7.51	57.9	1.11
China	2,328	1,064	1,264	32.1	161	72.4	998	10.7
Cuba	8.06	4.01	4.05	0.23	0.36	0.29	3.17	0.04
Europe	940	440	500	10.4	120	63.3	307	9.40
Haiti	7.54	3.47	4.07	0.32	0.44	0.71	2.60	0.11
Iceland	2.98	1.35	1.64	0.04	0.37	0.10	1.13	0.01
India	945	444	501	11.7	40.5	46.1	403	6.84
Israel	12.8	6.92	5.90	0.13	0.75	1.01	4.00	0.15
Jamaica	2.27	1.02	1.24	0.00	0.03	0.24	0.98	0.04
Japan	178	99.3	78.7	0.34	7.48	9.63	61.3	1.43
Mauritius	1.79	0.65	1.14	0.07	0.08	0.33	0.65	0.05
Mideast	678	329	349	2.94	22.4	46.6	277	6.92
New Zealand	17.6	9.43	8.14	0.01	0.43	1.13	6.57	0.17
Philippines	40.5	19.6	20.9	0.41	1.89	4.11	14.5	0.61
Russia	236	97.1	139	2.31	39.3	12.0	85.8	1.78
South America	489	232	258	7.17	13.4	35.6	201	5.28
Southeast Asia	583	262	321	9.11	23.3	58.0	230	8.61
South Korea	155	83.0	72.2	0.51	7.11	8.40	56.2	1.25
Taiwan	94.9	43.8	51.2	1.37	3.90	5.61	40.3	0.83
United States	939.46	473	467	6.93	51.8	78.0	330.	11.6
Total	8,693	4,122	4,571	97.6	548	523	3,403	**77.6**

37.1% of the transportation electric load is used to produce, compress, and store H_2. Annual-average H_2 loads are from Ref. S1.

Table S12. Final (from LOADMATCH) 2050 total (existing plus new) nameplate capacities (GW) of WWS generators by world region needed to match power demand with supply and storage continuously over time. Also provided are 143-country totals for 2050 and installed as of 2018 end, the nameplate capacity (MW) per device, and the 143-country total number of existing plus new devices needed at that nameplate capacity. The nameplate capacity equals the maximum possible instantaneous discharge rate.

Region	Onshore wind	Off-shore wind	Resi-dential rooftop PV	Comm/ govt rooftop PV	Utility PV	CSP with stor-age	Geoth ermale lec-tricity	Hydrop ower	Wave	Tidal	Solar ther-mal heat	Geo-ther-mal heat
Africa	755	98.4	196	372	392	45.9	3.61	29.3	12.0	1.90	2.04	0.14
Australia	94.7	23.5	34.9	59.8	203	13.0	0.40	8.05	2.91	0.50	6.57	0.02
Canada	183	29.8	11.7	98.2	34.3	0.00	5.00	80.8	4.05	2.00	8.42	1.47
Central America	350	55.3	55.2	129	73.2	21.1	10.7	18.3	11.8	0.38	2.67	0.16
Central Asia	181	21.2	94.2	145	181	11.6	0	20.0	1.79	0.02	0	0
China	3,565	735	803	928	2,809	296	1.86	318	8.71	3.02	351	17.9
Cuba	15.6	4.09	3.51	9.43	5.84	1.71	0	0.06	0.23	0.05	0	0.00
Europe	1,257	395	317	507	1,106	21.1	3.17	167	15.5	15.0	36.7	22.3
Haiti	2.48	4.52	2.17	8.83	5.97	0.63	0.68	0.60	0	0.05	0	0
Iceland	1.19	0	0	0	0	0	0.89	1.99	0.04	0.06	0	2.04
India	978	99.5	67.4	1,159	3,159	233	0.28	47.3	5.06	0.72	7.76	0.99
Israel	2.60	5.42	1.16	14.6	56.7	1.99	0	0.01	0	0.01	3.50	0.08
Jamaica	0.38	1.79	2.27	2.49	2.89	0.28	0	0.02	0	0.02	0	0
Japan	10.9	282	21.8	14.2	534	0	1.46	22.3	12.70	2.20	2.54	2.19
Mauritius	0.09	2.50	0.39	0.25	1.80	0.08	0	0.06	0.06	0.01	0	0.00
Mideast	1,004	140	245	315	1,467	117	1.41	44.7	1.92	0.28	16.3	3.17
New Zealand	21.8	1.75	5.32	6.62	16.9	1.16	2.00	5.35	0.41	0.20	0	0.49
Philippines	17.0	18.3	23.7	52.0	52.7	2.94	5.73	3.63	1.95	0.50	0	0
Russia	499	45.3	67.9	89.8	243	3.24	0.50	50.2	4.92	0.36	0	0.38
South America	1,304	106	118	256	316	39.2	5.35	166	23.2	1.23	10.5	0.58
Southeast Asia	53.8	458	441	468	854.6	340	13.8	36.3	14.8	0.79	0	0.16
South Korea	2.16	255	107	114	353	24.0	0	6.49	0	1.00	0	0.84
Taiwan	4.48	114	32.1	57.5	130	0	33.6	2.09	1.05	0.03	1.27	0
United States	1,785	350	207	307	1,645	90.3	6.52	80.1	33.0	0.35	18.3	17.4
Total 2050	12,088	3,246	2,858	5,113	13,643	1,265	97	1,109	156	31	467	70.3
Total 2018	571	24.6	95.6	95.6	287	5.47	13.3	1,109	0	0.54	459	70.3
Device MW	5	5	0.005	0.1	50	100	100	1,300	1	1	50	50.00
Device number	2,417,530	649,278	571,627,608	51,128,621	272,851	12,650	970	853	208,314	30,614	9,341	1,407

Device MW = the nameplate capacity of one device in megawatts. Device number is the number of all devices among 143 countries of the given nameplate capacity per device, in 2050.

Table S13. LOADMATCH capacity adjustment factors (CAFs), which show the ratio of the final nameplate capacity of several generators to meet load continuously, after running LOADMATCH, to the pre-LOADMATCH initial nameplate capacity estimated herein (e.g., Table 3 of Ref. S1) to meet load in the annual average. Thus, a CAF less than 1.0 means that the LOADMATCH-stabilized grid meeting hourly demand requires less than the nameplate capacity needed to meet annual average load (which is our initial, pre-LOADMATCH nameplate-capacity assumption). Column (f) is the ratio of CSP turbine nameplate capacity (CSP storage maximum discharge rate) needed to keep the grid stable here relative to the pre-LOADMATCH nameplate capacity estimate for annual average power plus for keeping the grid stable. The pre-LOADMATCH factor is 1.6 (thus an estimated 60% more CSP turbines were added to keep the grid stable). Thus, a number less than 1.6 here indicates fewer CSP turbines are needed compared with the pre-LOADMATCH estimate. Table S12 provides the final CSP nameplate capacity, accounting for this factor. All generators not on this list have a CAF = 1.

Region	(a) Onshore wind CAF	(b) Off-shore wind CAF	(c) Res. Roof PV CAF	(d) Com./Gov Roof PV CAF	(e) Utility PV CAF	(f) CSP turbine factor	(g) Solar Thermal CAF
Africa	1.27	0.8	0.7	0.7	0.9	1	0.01
Australia	1.18	0.7	0.75	0.75	1.95	1.6	0.181
Canada	1.4	0.9	0.2	0.7	0.5	0	0.2
Central America	1.35	1	0.85	0.88	0.98	1.6	0.06
Central Asia	1.41	0.9	0.85	0.85	1	1	0
China	1.75	0.7	0.55	0.55	1.7	1.4	0.464
Cuba	1.5	1.5	1	1.2	1.45	2.4	0
Europe	1.45	1	0.68	0.9	1	1	0.109
Haiti	0.4	1.55	0.5	1	1.2	1	0
Iceland	0.4	0.04	0	0	0	0	0
India	1.05	0.6	0.1	1.3	3	2.59	0.019
Israel	1	0.88	0.1	2.3	2.7	1.9	0.571
Jamaica	0.8	0.95	0.9	1	1	1.2	0
Japan	0.2	2	0.2	0.2	2	0	0.036
Mauritius	0.85	1.95	0.2	0.2	0.8	0.5	0
Mideast	2.1	0.8	0.75	0.75	1.38	2	0.057
New Zealand	1.49	0.4	0.6	0.6	1.65	0.8	0
Philippines	1.35	0.85	0.9	0.9	1.75	0.9	0
Russia	2	0.6	0.45	0.45	1.5	0.7	0
South America	1.25	0.75	0.6	0.6	1.28	1	0.077
Southeast Asia	0.2	0.65	0.88	0.88	1.3	7	0
South Korea	0.1	1.4	1.5	2.5	1.2	1.6	0
Taiwan	0.6	1.8	0.7	2.5	1.21	0	0.046
United States	1.7	0.8	0.45	0.45	2.4	1.7	0.064

Table S14. Average 2050 capacity factors (percent of nameplate capacity produced as electricity before transmission, distribution or maintenance losses) by region in this study.

Region	Onshore wind	Off-shore wind	Rooftop PV	Utility PV	CSP with storage	Geo-thermal elec-tricity	Hydr opow er	Wave	Tidal	Solar therm al	Geo-thermal heat
Africa	0.364	0.422	0.211	0.226	0.826	0.809	0.697	0.201	0.226	0.117	0.974
Australia	0.418	0.532	0.215	0.253	0.889	0.904	0.696	0.332	0.247	0.118	0.974
Canada	0.382	0.462	0.197	0.200	--	0.862	0.628	0.297	0.236	0.108	0.973
Central America	0.240	0.309	0.222	0.255	0.891	0.840	0.639	0.126	0.230	0.124	0.973
Central Asia	0.442	0.484	0.201	0.221	0.748	--	0.702	0.121	0.216	--	0.966
China	0.361	0.331	0.196	0.223	0.744	0.896	0.691	0.139	0.236	0.108	0.973
Cuba	0.278	0.347	0.227	0.254	0.896	--	0.609	0.379	0.232	--	--
Europe	0.364	0.447	0.196	0.205	0.801	0.861	0.619	0.237	0.237	0.106	0.973
Haiti	0.226	0.464	0.226	0.258	0.919	0.877	0.879	--	0.216	--	--
Iceland	0.491	0.625	--	--	--	0.925	0.683	0.317	0.252	--	0.973
India	0.286	0.341	0.194	0.233	0.819	0.857	0.919	0.133	0.234	0.109	0.973
Israel	0.360	0.346	0.236	0.265	0.904	--	0.550	--	0.252	0.131	0.974
Jamaica	0.291	0.476	0.234	0.265	0.948	--	0.410	--	0.208	--	--
Japan	0.295	0.439	0.166	0.183	--	0.909	0.488	0.141	0.249	0.091	0.973
Mauritius	0.563	0.604	0.211	0.232	0.799	--	0.483	0.318	0.251	--	--
Mideast	0.439	0.389	0.226	0.237	0.827	0.798	0.574	0.135	0.233	0.124	0.973
New Zealand	0.469	0.601	0.192	0.210	0.698	0.885	0.522	0.353	0.242	--	0.973
Philippines	0.210	0.325	0.230	0.260	0.946	0.858	0.532	0.133	0.235	--	0.983
Russia	0.351	0.465	0.188	0.206	0.673	0.863	0.495	0.256	0.237	--	0.973
South America	0.192	0.450	0.214	0.225	0.776	0.883	0.616	0.151	0.239	0.119	0.973
Southeast Asia	0.084	0.144	0.191	0.207	0.728	0.879	0.738	0.192	0.227	--	0.974
South Korea	0.284	0.432	0.173	0.163	0.522	--	0.569	--	0.251	--	0.973
Taiwan	0.187	0.346	0.192	0.214	0.001	0.927	0.611	0.144	0.255	0.107	--
United States	0.319	0.330	0.216	0.228	0.856	0.892	0.677	0.294	0.244	0.116	0.973
Average	**0.322**	**0.364**	**0.201**	**0.221**	**0.775**	**0.870**	**0.681**	**0.182**	**0.236**	**0.112**	**0.974**

Capacity factors of offshore and onshore wind turbines account for array losses (extraction of kinetic energy by turbines). In all cases, capacity factors are before transmission, distribution, and maintenance losses, which are given in Table S7. The average is weighted by nameplate capacity (Table S12). The symbol "--" indicates no installation of the technology. Rooftop PV panels are fixed-tilt at the optimal tilt angle of the country they reside in; utility PV panels are half fixed optimal tilt and half single-axis horizontal tracking[31].

Table S15. Aggregate (among all storage devices in a country or region) maximum instantaneous charge rates, maximum instantaneous discharge rates, and maximum energy storage capacities of the different types of electricity storage (PHS, CSP-PCM, batteries, hydropower), cold storage (CW-STES, ICE), and heat storage (HW-STES, UTES) technologies treated here, by region. Table S16 gives the maximum number of hours of storage at the maximum discharge rate. The product of the maximum discharge rate and hours of storage gives the maximum energy storage capacity.

	Africa			**Australia**			**Canada**			**Central America**		
Storage technology	Max charge rate GW	Max dis-charge rate GW	Max stor-age capac-ity TWh	Max charge rate GW	Max dis-charge rate GW	Max stor-age capac-ity TWh	Max charge rate GW	Max dis-charge rate GW	Max stor-age capac-ity TWh	Max charge rate GW	Max dis-charge rate GW	Max stor-age capac-ity TWh
PHS	27.8	27.8	0.389	10.7	10.7	0.150	16.6	16.6	0.233	6.0	6.0	0.084
CSP-elec.	45.9	45.9	--	13.0	13.0	--	0	0	--	21.1	21.1	--
CSP-PCM	74.1	--	1.037	21.0	--	0.293	0	--	0	34.0	--	0.476
Batteries	1,200	1,200	2.33	500	500	0.97	100	100	0.194	280.0	280.0	0.543
Hydropower	12.4	29.3	109	3.74	8.05	32.7	35.8	80.8	313	7.81	18.3	68.4
CW-STES	3.7	3.7	0.051	0.150	0.15	0.002	0.192	0.192	0.0027	0.49	0.49	0.007
ICE	5.5	5.5	0.077	0.23	0.23	0.003	0.288	0.288	0.004	0.74	0.74	0.010
HW-STES	129	129	1.04	8.99	8.99	0.072	19.1	19.1	0.268	26.2	26.2	0.210
UTES-heat	2.04	129	62.1	6.57	8.99	1.08	8.42	19.1	4.58	2.7	26.2	0.629
UTES-elec.	388	--	--	27.0	--	--	38.2	--	--	78.6	--	--
	Central Asia			**China**			**Cuba**			**Europe**		
PHS	12.0	12.0	0.168	116	116	1.62	3.0	3.0	0.042	197	197	2.76
CSP-elec.	11.6	11.6	--	296	296	--	1.7	1.7	--	21.1	21.1	--
CSP-PCM	18.7	--	0.262	478	--	6.69	2.8	--	0.039	34.0	--	0.475
Batteries	800	800	1.55	2,600	2,600	5.04	190	190	0.369	1,400	1,400	2.72
Hydropower	8.4	20.0	73.7	146	318	1,279	0.03	0.064	0.245	75.8	167.4	664
CW-STES	0.1	0.1	0.001	12.8	12.8	0.18	0.093	0.093	0.001	4.17	4.17	0.058
ICE	0.15	0.15	0.002	19.2	19.2	0.269	0.14	0.14	0.002	6.25	6.25	0.088
HW-STES	28.3	28.3	0.227	528	528	2.64	5.85	5.85	0.047	301	301	1.81
UTES-heat	0.0	28.3	23.8	351	528	342	0.0	5.85	0.421	36.7	301	145
UTES-elec.	28.3	--	--	1,056	--	--	17.5	--	--	452	--	--
	Haiti			**Iceland**			**India**			**Israel**		
PHS	2.0	2.0	0.028	0	0	0	28.8	28.8	0.403	10	10	0.14
CSP-elec.	0.63	0.63	--	0	0	--	233	233	--	1.99	1.99	--
CSP-PCM	1.01	--	0.014	0	--	0	375	--	5.26	3.20	--	0.045
Batteries	280	280	0.543	0	0	0	6,990	6,990	13.6	250	250	0.485
Hydropower	0.27	0.60	2.34	0.944	1.97	8.27	20.7	47.3	181	0.003	0.007	0.029
CW-STES	0.13	0.13	0.002	0.017	0.017	0.0002	4.7	4.7	0.066	0.054	0.054	0.001
ICE	0.19	0.19	0.003	0.025	0.025	0.0004	7.0	7.0	0.099	0.080	0.080	0.001
HW-STES	0	0	0	0.616	0.616	0.005	362	362	2.90	2.99	2.99	0.0239
UTES-heat	0	0.90	2.48	0	0.616	0	7.76	362	78.3	3.5	2.99	1.08
UTES-elec.	13.8	--	--	0	--	--	1,087	--	--	8.98	--	--
	Jamaica			**Japan**			**Mauritius**			**Mideast**		
PHS	3.00	3.00	0.042	177	177	2.47	40.0	40.0	0.560	14.5	14.5	0.203
CSP-elec.	0.28	0.28	--	0	0	--	0.078	0.078	--	117	117	--
CSP-PCM	0.45	--	0.006	0	--	0	0.126	--	0.002	189	--	2.65
Batteries	40.0	40.0	0.078	590	590	1.15	5.00	5.00	0.010	2,400	2,400	4.66
Hydropower	0.01	0.02	0.080	10.4	22.3	91.1	0.028	0.06	0.247	18.7	44.7	164
CW-STES	0	0	0	0.13	0.13	0.002	0.03	0.03	0.0004	1.2	1.2	0.016
ICE	0	0	0	0.20	0.20	0.003	0.044	0.044	0.0006	1.8	1.8	0.025
HW-STES	1.22	1.22	0.01	20.2	20.2	0.161	0	0	0	81.0	81.0	0.648
UTES-heat	0.00	1.22	0.15	2.5	20.1	2.42	0	1.55	0.186	16.2	81.0	19.4
UTES-elec.	0.37	--	--	60.5	--	--	3.10	--	--	243	--	--
	New Zealand			**Philippines**			**Russia**			**South America**		
PHS	6.00	6.00	0.084	22.4	22.4	0.314	20.8	20.8	0.292	19.5	19.5	0.273
CSP-elec.	1.16	1.16	--	2.9	2.9	--	3.2	3.2	--	39.2	39.2	--

CSP-PCM	1.87	--	0.026	4.7	--	0.066	5.2	--	0.073	63.2	--	0.884
Batteries	140	140	0.272	80.0	80.0	0.155	40.0	40.0	0.078	10.0	10.0	0.019
Hydropower	2.43	5.35	21.3	1.6	3.6	14.0	22.4	50.2	196	73.3	166	643
CW-STES	0.005	0.005	0.0001	0.17	0.17	0.0023	0.92	0.92	0.013	2.9	2.9	0.040
ICE	0.007	0.007	0.0001	0.25	0.25	0.0035	1.4	1.4	0.019	4.3	4.3	0.060
HW-STES	1.03	1.03	0.0083	31.9	31.9	0.0255	92.0	92.0	0.92	54.9	54.9	0.44
UTES-heat	0	1.03	0.62	0	31.9	27.6	0	92.0	66.2	10.5	54.9	2.64
UTES-elec.	2.07	--	--	95.7	--	--	92.0	--	--	110	--	--
	Southeast Asia			**South Korea**			**Taiwan**			**United States**		
PHS	53.5	53.5	0.749	96.5	96.5	1.35	49.1	49.1	0.688	95.8	95.8	1.342
CSP-elec.	340	340	--	24.0	24.0	--	0	0	--	90.3	90.3	--
CSP-PCM	549	--	7.68	38.7	--	0.54	0	--	0	146	--	2.038
Batteries	950	950	1.84	2,800	2,800	5.43	1,750	1,750	3.40	2,700	2,700	5.24
Hydropower	15.9	36.3	140	3.1	6.5	26.9	1.0	2.1	8.71	36.7	80.1	321
CW-STES	3.64	3.64	0.051	0.20	0.20	0.003	0.55	0.55	0.008	2.8	2.8	0.039
ICE	5.46	5.46	0.077	0.31	0.31	0.004	0.82	0.82	0.012	4.2	4.2	0.058
HW-STES	208	208	1.66	22.8	22.8	0.183	25.2	25.2	0.201	154	154	1.23
UTES-heat	0	208	24.9	0	22.8	8.21	1.27	25.2	0.604	18.3	154	7.39
UTES-elec.	623	--	--	68.4	--	--	75.5	--	--	462	--	--

PHS = pumped hydropower storage; PCM = Phase-change materials; CSP=concentrated solar power; CW-STES = Chilled-water sensible heat thermal energy storage; HW-STES = Hot water sensible heat thermal energy storage; and UTES = Underground thermal energy storage (either boreholes, water pits, or aquifers). The peak energy storage capacity equals the maximum discharge rate multiplied by the maximum number of hours of storage at the maximum discharge rate. Table S16 gives maximum storage times at the maximum discharge rate.

Heat captured by CSP solar collectors can either be used immediately to produce electricity, put in storage, or both. The maximum direct CSP electricity production rate (CSP-elec) equals the maximum electricity discharge rate, which equals the nameplate capacity of the generator. The maximum charge rate of CSP phase-change material storage (CSP-PCM) is set to 1.612 multiplied by the maximum electricity discharge rate, which allows more energy to be collected than discharged directly. Thus, the maximum overall simultaneous direct electricity plus storage CSP production rate is 2.612 multiplied by the discharge rate. The maximum energy storage capacity equals the maximum electricity discharge rate multiplied by the maximum number of hours of storage at full discharge, set to 22.6 hours, or 1.612 multiplied by the 14 hours required for CSP storage to charge when charging at its maximum rate.

Hydropower can be charged only naturally, but its annual-average charge rate must equal at least its annual energy output divided by the number of hours per year. It is assumed simplistically here that hydro is recharged at that rate, where its annual energy output in 2050 is close to its current value. Hydropower's maximum discharge rate in 2050 is its 2018 nameplate capacity. The maximum storage capacity is set equal to the 2050 annual energy output of hydro.

The CW-STES charge/discharge rate is set equal to 40% of the maximum daily averaged cold load subject to storage. The ICE storage charge/discharge rate is set to 60% of the same peak cold load subject to storage.

The HW-STES charge and discharge rates are set equal to the maximum daily-averaged heat load subject to storage, calculated as the maximum value during the period of simulation.

UTES heat stored in underground soil can be charged by either solar or geothermal heat or excess electricity. The maximum charge rate of heat to UTES storage (UTES-heat) is set to the nameplate capacity of the solar thermal collectors. In several regions, no solar thermal collectors are used. Instead, UTES is charged only with excess grid electricity. The maximum charge rate of excess grid electricity converted to heat stored in UTES (UTES-elec.) is set by trial and error for each country. The maximum UTES heat discharge rate is set to that of HW-STES storage, which is limited by the warm storage load.

Table S16. Maximum number of hours or days of storage at the maximum discharge rate of each storage type (given in Table S15 for each region). The maximum discharge rate multiplied by the number of hours of storage equals the maximum storage capacity in Table S15. For all regions, the maximum CSP storage time at the maximum discharge rate is 22.6 h; that for PHS storage is 14 h; that for ICE storage is 14 h; and that for battery storage is 1.94 h.

Region	HW-, CW-STES (hours)	UTES (day)	H_2 (day)
Africa	8	20	1
Australia	8	5	3
Canada	14	10	0
Central America	8	1	15
Central Asia	8	35	3
China	5	27	7
Cuba	8	3	30
Europe	6	20	5
Haiti	8	15	15
Iceland	8	0	1
India	8	9	6
Israel	8	15	20
Jamaica	8	5	5
Japan	8	5	5
Mauritius	8	5	25
Mideast	8	10	10
New Zealand	8	25	3
Philippines	8	36	15
Russia	10	30	5
South America	8	2	1
Southeast Asia	8	5	3
South Korea	8	15	15
Taiwan	8	1	40
United States	8	2	20

Table S17. Budgets of WWS end-use energy demand met, energy losses, energy supplies, and changes in storage, during the 1-year (8,747.4875 hour) simulations for all 24 world regions and the sum of results for all regions. All units are TWh over the 1-year simulation. Divide TWh by the number of hours of simulation to obtain annual-average power values (TW). Table S5 identifies the countries within each region. Figure S2 shows the time series of matching demand with supply and changes in storage for each region.

	Africa	Australia	Canada	Central America	Central Asia
A1. Total end use demand	**4,214**	**819**	**1,326**	**1,351**	**1,322**
Electricity for electricity inflexible demand	2,072	430	698	632	695
Electricity for electricity, heat, cold storage + DR	1,787	329	553	581	561
Electricity for H_2 direct use + H_2 storage	355	60	75	137	66
A2. Total end use demand	**4,214**	**819**	**1,326**	**1,351**	**1,322**
Electricity for direct use, electricity storage, + H_2	3,924	791	1,267	1,300	1,267
Low-T heat load met by heat storage	264	26	58	47	54
Cold load met by cold storage	26.29	0.87	0.36	3.39	0.52
A3. Total end use demand	**4,214**	**819**	**1,326**	**1,351**	**1,322**
Electricity for direct use, electricity storage, DR	3,515	729	1,170	1,155	1,200
Electricity for H_2 direct use + H_2 storage	355	60	75	137	66
Electricity + heat for heat subject to storage	264	26	77	47	54
Electricity for cold load subject to storage	80.22	3.28	4.19	10.81	2.18
B. Total losses	**985**	**427**	**160**	**415**	**449**
Transmission, distribution, downtime losses	323	83	100	111	107
Losses CSP storage	1.54	0.46	0	0.51	0.45
Losses PHS storage	15.2	6.3	5.8	2.6	8.1
Losses battery storage	20	2.4	0.02	3.5	7.7
Losses CW-STES + ICE storage	5	0.2	0.07	0.6	0.1
Losses HW-STES storage	34	3.9	8	9.4	6.4
Losses UTES storage	61	4.5	12	0.5	15.7
Losses from shedding	525	326	35	287	303
Net end-use demand plus losses (A1 + B)	***5,199***	***1,245***	***1,485***	***1,766***	***1,771***
C. Total WWS supply before T&D losses	**5,151**	**1,246**	**1,483**	**1,767**	**1,762**
Onshore + offshore wind electricity	2,767	455	732	885	790
Rooftop + utility PV+ CSP electricity	2,154	727	250	685	847
Hydropower electricity	179	49	444	102	123
Wave electricity	21	8	11	13	2
Geothermal electricity	25.5	3.16	37.7	78.6	0
Tidal electricity	3.75	1.08	4.12	0.765	0.039
Solar heat	0.519	1.70	1.99	0.723	0
Geothermal heat	0.292	0.034	3.121	0.35	0.007
D. Net taken from (+) or added to (-) storage	**48.2**	**-0.226**	**2.173**	**-0.761**	**8.282**
CSP storage	0.535	0.032	0	-0.048	0.196
PHS storage	0.35	0.088	-0.042	-0.008	0.126
Battery storage	0.769	-0.136	-0.049	-0.054	0.052
CW-STES+ICE storage	0.116	0.004	-0.002	-0.002	0
HW-STES storage	0.932	-0.004	0.201	-0.021	0.17
UTES storage	44.7	-0.27	2.06	-0.063	7.25
H_2 storage	0.876	0.06	0	-0.565	0.486
Energy supplied plus taken from storage (C+D)	***5,199***	***1,245***	***1,485***	***1,766***	***1,771***

	China	Cuba	Europe	Haiti	Iceland
A1. Total end use demand	**20,366**	**71**	**8,221**	**66**	**26**
Electricity for electricity inflexible demand	9,496	37	3,948	33	12

Electricity for electricity, heat, cold storage + DR	10,237	32	3,720	27	13
Electricity for H_2 direct use + H_2 storage	633	3	554	6	1
A2. Total end use demand	**20,366**	**71**	**8,221**	**66**	**26**
Electricity for direct use, electricity storage, + H_2	18,894	67	7,203	62	22
Low-T heat load met by heat storage	1,412	3	1,004	4	3
Cold load met by cold storage	60.31	0.62	14.04	0.23	0.00
A3. Total end use demand	**20,366**	**71**	**8,221**	**66**	**26**
Electricity for direct use, electricity storage, DR	18,041	63	6,531	53	22
Electricity for H_2 direct use + H_2 storage	633	3	554	6	1
Electricity + heat for heat subject to storage	1,412	3	1,045	4	3
Electricity for cold load subject to storage	280.55	2.04	91.10	2.81	0.00
B. Total losses	**5,703**	**33**	**2,034**	**10**	**3**
Transmission, distribution, downtime losses	1,755	6	675	4	2
Losses CSP storage	9.90	0.04	0.48	0.03	0.00
Losses PHS storage	57.8	1.1	80.1	1.3	0.0
Losses battery storage	42	0.46	9	1.1	0.00
Losses CW-STES + ICE storage	11	0.11	3	0.0	0.00
Losses HW-STES storage	152	0.49	145	0.0	0.01
Losses UTES storage	368	0.41	153	2.3	0.00
Losses from shedding	3,306	24	968	0.8	0.9
Net end-use demand plus losses (A1 + B)	***26,069***	***103***	***10,255***	***75.8***	***28.8***
C. Total WWS supply before T&D losses	**25,821**	**104**	**10,134**	**74**	**29**
Onshore + offshore wind electricity	13,379	50	5,540	23	5
Rooftop + utility PV+ CSP electricity	10,369	52	3,545	40	0
Hydropower electricity	1,921	0	906	5	12
Wave electricity	11	1	32	0	0
Geothermal electricity	14.6	0	23.9	5.21	7.20
Tidal electricity	6.217	0.096	30.991	0.099	0.125
Solar heat	82.5	0	8.51	0	0
Geothermal heat	38.1	0	47.5	0	4.34
D. Net taken from (+) or added to (-) storage	**248**	**-0.106**	**121**	**2.21**	**-0.001**
CSP storage	1.23	-0.002	-0.048	0.002	0
PHS storage	-0.114	-0.002	-0.276	0.013	0
Battery storage	-0.504	-0.037	-0.272	-0.02	0
CW-STES+ICE storage	-0.045	0.002	-0.015	0.004	0
HW-STES storage	2.374	-0.004	-0.181	0	-0.002
UTES storage	240	-0.042	115	1.98	0
H_2 storage	5.193	-0.02	6.598	0.232	0.002
Energy supplied plus taken from storage (C+D)	***26,069***	***103***	***10,255***	***75.8***	***28.8***

	India	Israel	Jamaica	Japan	Mauritius
A1. Total end use demand	**8,267**	**112**	**20**	**1,557**	**16**
Electricity for electricity inflexible demand	3,949	62	9	873	6
Electricity for electricity, heat, cold storage + DR	3,914	42	9	599	7
Electricity for H_2 direct use + H_2 storage	403	9	2	84	3
A2. Total end use demand	**8,267**	**112**	**20**	**1,557**	**16**
Electricity for direct use, electricity storage, + H_2	7,886	106	20	1,494	15
Low-T heat load met by heat storage	354	6	0	62	1
Cold load met by cold storage	25.93	0.26	0.00	0.48	0.22
A3. Total end use demand	**8,267**	**112**	**20**	**1,557**	**16**
Electricity for direct use, electricity storage, DR	7,407	96	18	1,404	11
Electricity for H_2 direct use + H_2 storage	403	9	2	84	3

Electricity + heat for heat subject to storage	354	7	0	65	1
Electricity for cold load subject to storage	102.73	1.17	0.00	2.94	0.65
B. Total losses	**5,065**	**95**	**7**	**596**	**4**
Transmission, distribution, downtime losses	874	13	1	158	1
Losses CSP storage	10.68	0.09	0.01	0.00	0.00
Losses PHS storage	22.3	5.8	0.9	34.8	0.3
Losses battery storage	162	1	0.01	0.40	0.00
Losses CW-STES + ICE storage	5	0	0.00	0.09	0.04
Losses HW-STES storage	54	1	0.03	6.97	0.00
Losses UTES storage	68	2	0.07	17.26	0.46
Losses from shedding	3,869	73	5	378	2
Net end-use demand plus losses (A1 + B)	***13,331***	***207***	***27.3***	***2,153***	***19.6***
C. Total WWS supply before T&D losses	**13,328**	**205**	**27**	**2,149**	**19**
Onshore + offshore wind electricity	2,741	25	8	1,112	14
Rooftop + utility PV+ CSP electricity	10,193	180	19	905	5
Hydropower electricity	380	0	0	95	0
Wave electricity	6	0	0	16	0
Geothermal electricity	2.10	0	0	11.7	0
Tidal electricity	1.48	0.019	0.037	4.78	0.014
Solar heat	1.86	1	0	0.505	0
Geothermal heat	2.11	0.175	0	4.65	0
D. Net taken from (+) or added to (-) storage	**3.88**	**1.97**	**-0.03**	**3.56**	**0.129**
CSP storage	2.42	0.032	0	0	0.001
PHS storage	0.382	0.126	-0.003	0.129	-0.053
Battery storage	2.48	0.382	-0.008	0.062	-0.001
CW-STES+ICE storage	0.029	0.002	0	0.003	0.001
HW-STES storage	2.59	0.022	-0.001	0.145	0
UTES storage	-3.91	0.97	-0.015	2.18	0.006
H_2 storage	-0.102	0.438	-0.003	1.04	0.176
Energy supplied plus taken from storage (C+D)	***13,331***	***207***	***27.3***	***2,153***	***19.6***

	Mideast	New Zealand	Philip-pines	Russia	South America
A1. Total end use demand	**5,928**	**154**	**354**	**2,068**	**4,278**
Electricity for electricity inflexible demand	2,890	83	174	865	2,057
Electricity for electricity, heat, cold storage + DR	2,630	61	144	1,098	1,910
Electricity for H_2 direct use + H_2 storage	408	10	36	105	311
A2. Total end use demand	**5,928**	**154**	**354**	**2,068**	**4,278**
Electricity for direct use, electricity storage, + H_2	5,725	150	336	1,724	4,134
Low-T heat load met by heat storage	196	4	17	340	117
Cold load met by cold storage	7.26	0.02	1.05	4.90	27.78
A3. Total end use demand	**5,928**	**154**	**354**	**2,068**	**4,278**
Electricity for direct use, electricity storage, DR	5,299	140	298	1,599	3,788
Electricity for H_2 direct use + H_2 storage	408	10	36	105	311
Electricity + heat for heat subject to storage	196	4	17	343	117
Electricity for cold load subject to storage	25.69	0.11	3.62	20.19	62.69
B. Total losses	**3,645**	**46**	**86**	**644**	**887**
Transmission, distribution, downtime losses	651	14	24	184	345
Losses CSP storage	2.74	0.03	0.13	0.03	1.23
Losses PHS storage	5.2	1.6	12.7	4.2	12.2
Losses battery storage	10.45	0.08	0.83	0.04	0.18

Losses CW-STES + ICE storage	1.31	0.00	0.19	0.89	5.01
Losses HW-STES storage	32.19	0.41	3.31	53.49	20.65
Losses UTES storage	22.76	0.63	1.21	45.03	9.62
Losses from shedding	2,919	29	43	356	493
Net end-use demand plus losses (A1 + B)	***9,573***	***199***	***440***	***2,712***	***5,165***
C. Total WWS supply before T&D losses	**9,573**	**199**	**443**	**2,664**	**5,165**
Onshore + offshore wind electricity	4,335	99	83	1,714	2,606
Rooftop + utility PV+ CSP electricity	4,991	58	296	716	1,588
Hydropower electricity	224	24	17	217	893
Wave electricity	2	1	2	11	31
Geothermal electricity	9.86	15.5	43.0	3.78	41.3
Tidal electricity	0.578	0.423	1.03	0.743	2.57
Solar heat	4.40	0	0	0	2.74
Geothermal heat	6.74	1.04	0.007	0.812	1.24
D. Net taken from (+) or added to (-) storage	**-0.661**	**-0.109**	**-2.81**	**48.42**	**-0.17**
CSP storage	0.868	-0.003	0.026	-0.004	-0.025
PHS storage	0.127	-0.008	0.04	-0.073	0.039
Battery storage	-0.428	-0.027	-0.016	-0.019	-0.002
CW-STES+ICE storage	-0.003	0	0.005	-0.008	0.09
HW-STES storage	0.583	-0.001	-0.025	0.181	-0.037
UTES storage	-1.18	-0.062	-2.76	47.3	-0.264
H_2 storage	-0.631	-0.008	-0.088	1.063	0.029
Energy supplied plus taken from storage (C+D)	***9,573***	***199***	***440***	***2,712***	***5,165***

	Southeast Asia	South Korea	Taiwan	United States	All Regions
A1. Total end use demand	**5,102**	**1,357**	**830**	**8,218**	**76,041**
Electricity for electricity inflexible demand	2,343	734	393	4,178	36,668
Electricity for electricity, heat, cold storage + DR	2,251	550	388	3,357	34,801
Electricity for H_2 direct use + H_2 storage	508	73	49	683	4,572
A2. Total end use demand	**5,102**	**1,357**	**830**	**8,218**	**76,041**
Electricity for direct use, electricity storage, + H_2	4,875	1,300	796	7,757	71,116
Low-T heat load met by heat storage	204	56	33	449	4,714
Cold load met by cold storage	22.55	0.98	1.66	11.77	211
A3. Total end use demand	**5,102**	**1,357**	**830**	**8,218**	**76,041**
Electricity for direct use, electricity storage, DR	4,311	1,217	735	7,022	65,822
Electricity for H_2 direct use + H_2 storage	508	73	49	683	4,572
Electricity + heat for heat subject to storage	204	62	34	453	4,793
Electricity for cold load subject to storage	79.66	4.46	11.96	60.63	854
B. Total losses	**1,149**	**608**	**201**	**3,356**	26,605
Transmission, distribution, downtime losses	375	126	68	810	6,814
Losses CSP storage	15.01	0.65	0.00	2.00	46
Losses PHS storage	34.3	29.6	20.0	40.4	403
Losses battery storage	12.32	6.50	3.41	37	320
Losses CW-STES + ICE storage	4.06	0.18	0.30	2	38
Losses HW-STES storage	28.49	5.57	5.77	75	646
Losses UTES storage	42.32	19.1	3.21	36	886
Losses from shedding	637	420	100	2,353	17,453
Net end-use demand plus losses (A1 + B)	***6,250***	***1,965***	***1,031***	***11,574***	***102,646***
C. Total WWS supply before T&D losses	**6,217**	**1,951**	**1,032**	**11,579**	**102,121**
Onshore + offshore wind electricity	617	969	352	5,999	45,301

Rooftop + utility PV+ CSP electricity	5,233	946	394	4,928	49,120
Hydropower electricity	234	32	11	474	6,344
Wave electricity	25	0	1	85	279
Geothermal electricity	106	0	272	50.8	752
Tidal electricity	1.56	2.20	0.06	0.746	63.5
Solar heat	0	0	0.296	4.64	111
Geothermal heat	0.345	1.78	0	37.1	150
D. Net taken from (+) or added to (-) storage	**33.8**	**14.2**	**-0.481**	**-5.35**	**525**
CSP storage	3.88	0.302	0	-0.203	9.18
PHS storage	0.712	0.149	0.167	-0.134	1.74
Battery storage	0.645	3.51	-0.17	-0.524	5.63
CW-STES+ICE storage	0.121	0.005	0.004	-0.01	0.30
HW-STES storage	1.58	0.164	-0.001	-0.067	8.60
UTES storage	23.1	7.39	-0.03	-0.739	482
H_2 storage	3.76	2.72	-0.451	-3.67	17.1
Energy supplied plus taken from storage (C+D)	***6,250***	***1,965***	***1,031***	***11,574***	***102,646***

End-use demands in A1, A2, A3 should be identical. Table S6 gives round-trip storage efficiencies. Table S7 gives transmission/distribution/maintenance losses. Generated electricity is shed when it exceeds the sum of electricity demand, cold storage capacity, heat storage capacity, and H_2 storage capacity. Onshore and offshore wind turbines in GATOR-GCMOM are assumed to be Senvion (formerly Repower) 5 MW turbines with 126-m diameter rotors, 100 m hub heights, a cut-in wind speed of 3.5 m/s, and a cut-out wind speed of 30 m/s. Rooftop PV panels in GATOR-GCMOM are modeled as fixed-tilt panels at the optimal tilt angle of the country they resided in; utility PV panels are modeled as half fixed optimal tilt and half single-axis horizontal tracking. All panels are assumed to have a nameplate capacity of 390 W and a panel area of 1.629668 m^2, which gives a 2050 panel efficiency (Watts of power output per Watt of solar radiation incident on the panel) of 23.9%, which is an increase from the 2015 value of 20.1%. Each CSP plant before storage is assumed to have the mirror and land characteristics of the Ivanpah solar plant, which has 646,457 m^2 of mirrors and 2.17 km^2 of land per 100 MW nameplate capacity and a CSP efficiency (fraction of incident solar radiation that is converted to electricity) of 15.796%, calculated as the product of the reflection efficiency of 55% and the steam plant efficiency of 28.72%. The efficiency of the solar thermal for heat hot fluid collection (energy in fluid divided by incident radiation) is assumed to be 34%.

Table S18. Summary, over 143 countries, of private and social costs. This is the 2050 143-country (24-world-region) WWS versus BAU mean social cost per unit energy. Also shown is the WWS-to-BAU aggregate social cost ratio and the components of its derivation.

a) BAU electricity private cost per unit energy (¢/kWh)[1]	9.99
b) BAU health cost per unit energy (¢/kWh)	16.9
c) BAU climate cost per unit energy (¢/kWh)	16.0
d) BAU social cost per unit energy (¢/kWh) (a+b+c)	**42.9**
e) WWS private and social cost per unit energy (¢/kWh)[1]	**8.94**
f) BAU end-use power demand (GW)[2]	20,255
g) WWS end-use power demand (GW)[2]	8,693
h) BAU electricity sector aggregate annual energy private cost ($tril/yr) (af)	17.7
i) BAU health cost ($tril/yr) (bf)	30.0
j) BAU climate cost ($tril/yr) (cf)	28.4
k) BAU social cost ($tril/yr) (df)	**76.1**
l) WWS private and social cost ($tril/yr) (eg)	**6.81**
m) WWS-to-BAU energy private cost/kWh ratio ($R_{WWS:BAU-E}$) (e/a)	0.90
n) BAU-energy-private-cost/kWh-to-BAU-social-cost/kWh ratio ($R_{BAU-S:E}$) (a/d)	0.23
o) WWS-kWh-used-to-BAU-kWh-used ratio ($R_{WWS:BAU-C}$) (g/f)	0.43
WWS-to-BAU aggregate social cost ratio (R_{ASC}) (mno)	**0.09**
WWS-to-BAU aggregate private cost ratio (R_{APC}) (mo)	**0.38**
WWS-to-BAU social cost per unit energy ratio (R_{SCE}) (mn)	**0.21**

[1]This is the BAU all-energy cost of energy per unit energy and is assumed to equal the BAU electricity-sector cost of energy per unit energy. The WWS cost per unit energy is for all energy, which is almost all electricity (plus a small amount of direct heat).

[2]Multiply GW by 8,760 hr/yr to obtain GWh/yr.

Table S19. Footprint and spacing areas per MW of nameplate capacity and installed power densities for WWS electricity or heat generation technologies.

WWS technology	Footprint area (m^2/MW)	Spacing area (km^2/MW)	Installed power density (MW/km^2)
Onshore wind	3.22	0.051	19.8
Offshore wind	3.22	0.139	7.2
Wave device	700	0.033	30.3
Geothermal plant	3,290	0	304
Hydropower plant	502,380	0	2.0
Tidal turbine	290	0.004	250
Residential roof PV	5,230	0	191
Commercial/govt. roof PV	5,230	0	191
Solar PV plant	12,220	0	81.8
Utility CSP plant	29,350	0	34.1
Solar thermal for heat	1,430	0	700

The installed power density is the inverse of either the spacing or, if spacing is zero, the footprint of the technology. From Ref. S1. Spacing areas for onshore and offshore wind are from Ref. S4.

Table S20. Footprint and spacing areas. Footprint areas are for new utility PV farms, CSP plants, solar thermal plants for heat, geothermal plants for electricity and heat, and hydropower plants. Spacing areas are for new onshore wind turbines. Solar PV footprint can reside within onshore wind spacing areas.

Region	Region land area (km^2)	Footprint Area (km^2)	Spacing area (km^2)	Land footprint area as percentage of region land area (%)	Land spacing area as a percentage of region land area (%)
Africa	22,988,130	6,082	38,219	0.027	0.166
Australia	7,682,300	2,788	4,535	0.036	0.059
Canada	9,093,510	425	8,697	0.005	0.096
Central America	2,429,460	1,516	17,560	0.062	0.723
Central Asia	4,697,670	2,539	9,163	0.054	0.195
China	11,063,254	41,747	171,276	0.377	1.548
Cuba	106,440	121	793	0.114	0.745
Europe	5,671,860	13,207	55,688	0.233	0.982
Haiti	75,880	92	117	0.122	0.155
Iceland	100,250	0	61	0.000	0.061
India	3,179,250	45,238	48,057	1.423	1.512
Israel	21,640	743	131	3.435	0.604
Jamaica	10,830	43	14	0.398	0.133
Japan	364,560	6,123	372	1.680	0.102
Mauritius	2,040	24	4	1.183	0.185
Mideast	6,327,218	21,307	50,798	0.337	0.803
New Zealand	263,310	243	1,077	0.092	0.409
Philippines	298,170	737	845	0.247	0.284
Russia	16,446,360	3,063	25,417	0.019	0.155
South America	17,176,021	4,991	65,518	0.029	0.382
Southeast Asia	3,927,017	20,443	2,677	0.521	0.068
South Korea	97,350	4,959	45	5.094	0.047
Taiwan	36,193	1,682	193	4.646	0.533
United States	9,147,420	22,350	86,114	0.244	0.941
All regions	**121,206,133**	**200,463**	**587,371**	**0.165**	**0.485**

Spacing areas are areas between wind turbines needed to avoid interference of the wake of one turbine with the next. Such spacing area can be used for multiple purposes, including farmland, rangeland, open space, or utility PV. Footprint areas are the physical land areas, water surface areas, or sea floor surface areas removed from use for any other purpose by an energy technology. Rooftop PV is not included in the footprint calculation because it does not take up new land. Conventional hydro new footprint is zero because no new dams are proposed as part of these roadmaps. Offshore wind, wave, and tidal are not included because they don't take up new land. Table S19 gives the installed power densities assumed. Areas are given both as an absolute area and as a percentage of the region land area, which excludes inland or coastal water bodies. For comparison, the total area and land area of Earth are 510.1 and 144.6 million km^2, respectively.

Table S21. Estimated mean number of long-term, full-time construction and operation jobs per MW nameplate capacity of different electric power sources and storage types in the United States. A full-time job is a job that requires 2,080 hours per year of work. The job numbers include direct, indirect, and induced jobs.

Electric power generator	Construction Jobs/MW or Jobs/km	Operation Jobs/MW or Jobs/km
Onshore wind electricity	0.24	0.37
Offshore wind electricity	0.31	0.63
Wave electricity	0.15	0.57
Geothermal electricity	0.71	0.46
Hydropower electricity	0.14	0.30
Tidal electricity	0.16	0.61
Residential rooftop PV	0.88	0.32
Commercial/government rooftop PV	0.65	0.16
Utility PV electricity	0.24	0.85
CSP electricity	0.31	0.86
Solar thermal for heat	0.71	0.85
Geothermal heat	0.14	0.46
Pumped hydro storage (PHS)	0.77	0.3
CSP storage (CSP-PCM)	0.62	0.3
Battery storage	0.092	0.2
Chilled-water storage (CW-STES)	0.15	0.3
Ice storage (ICE)	0.15	0.3
Hot water storage (HW-STES)	0.15	0.3
Underground heat storage (UTES)	0.15	0.3
Hydrogen production and storage	0.32	0.3
AC transmission (jobs/km)	0.073	0.062
AC distribution (jobs/km)	0.033	0.028
HVDC transmission (jobs/km)	0.088	0.082

From Ref. S1. The number of full-time construction jobs is the number of 1-year jobs divided by the lifetime (in years) of the device (Table S7).

Supporting Figures

Figure S1. Modeled time-series of solar PV+CSP electricity production, onshore plus offshore wind energy production, building total cold load, and building total heat load (as used in LOADMATCH), summed over each region. The five time-series panels for each region are for the full year (2050) and for 10 days within each season, respectively. Results are shown hourly, so units are energy output (TWh) per hour increment, thus also units of power (TW) averaged over the hour. Raw GATOR-GCMOM results were provided and fed into LOADMATCH at 30 s time increments. LOADMATCH modified the magnitudes of GATOR-GCMOM results, as described in the main text. The last set of panels for each region includes correlation plots of building heat load versus wind power output; building cold load versus wind power output; and wind power output versus solar power output, obtained from all hourly data in the first panel. Table 3 of the main text summarizes the R values from these plots, as well as for plots of heat and cold load versus solar power output, for all regions. Table 1 shows the annual average building total cold (L_{cold}) and heat (L_{heat}) loads.

CENTRAL AMERICA

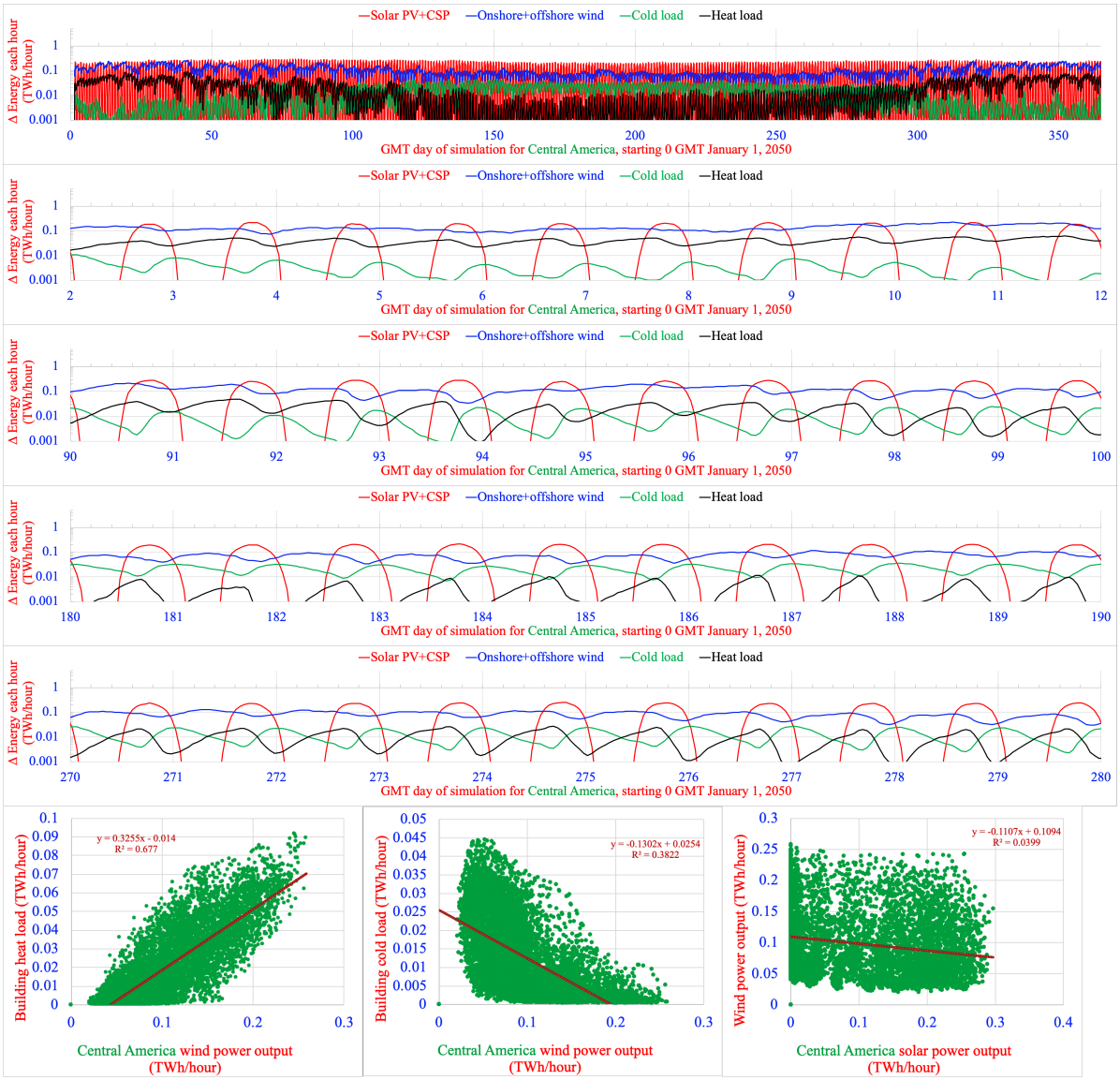

CHINA

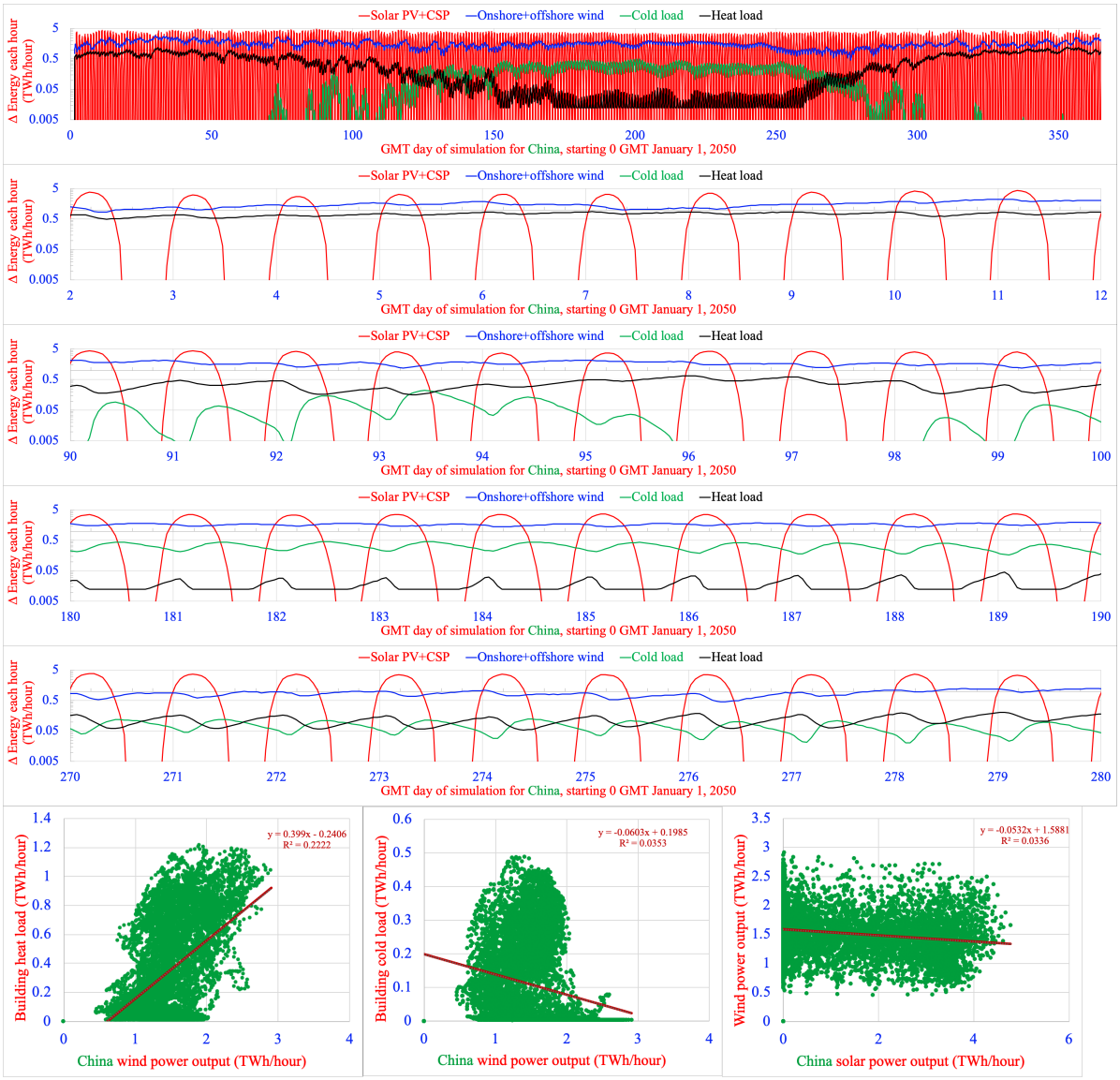
—Solar PV+CSP —Onshore+offshore wind —Cold load —Heat load
Δ Energy each hour (TWh/hour)
5
0.5
0.05
0.005
0 50 100 150 200 250 300 350
GMT day of simulation for China, starting 0 GMT January 1, 2050
—Solar PV+CSP —Onshore+offshore wind —Cold load —Heat load
Δ Energy each hour (TWh/hour)
5
0.5
0.05
0.005
2 3 4 5 6 7 8 9 10 11 12
GMT day of simulation for China, starting 0 GMT January 1, 2050
—Solar PV+CSP —Onshore+offshore wind —Cold load —Heat load
Δ Energy each hour (TWh/hour)
5
0.5
0.05
0.005
90 91 92 93 94 95 96 97 98 99 100
GMT day of simulation for China, starting 0 GMT January 1, 2050
—Solar PV+CSP —Onshore+offshore wind —Cold load —Heat load
Δ Energy each hour (TWh/hour)
5
0.5
0.05
0.005
180 181 182 183 184 185 186 187 188 189 190
GMT day of simulation for China, starting 0 GMT January 1, 2050
—Solar PV+CSP —Onshore+offshore wind —Cold load —Heat load
Δ Energy each hour (TWh/hour)
5
0.5
0.05
0.005
270 271 272 273 274 275 276 277 278 279 280
GMT day of simulation for China, starting 0 GMT January 1, 2050
Building heat load (TWh/hour)
y = 0.399x - 0.2406
R² = 0.2222
1.4 1.2 1 0.8 0.6 0.4 0.2 0
0 1 2 3 4
China wind power output (TWh/hour)
Building cold load (TWh/hour)
y = -0.0603x + 0.1985
R² = 0.0353
0.6 0.5 0.4 0.3 0.2 0.1 0
0 1 2 3 4
China wind power output (TWh/hour)
Wind power output (TWh/hour)
y = -0.0532x + 1.5881
R² = 0.0336
3.5 3 2.5 2 1.5 1 0.5 0
0 2 4 6
China solar power output (TWh/hour)

EUROPE

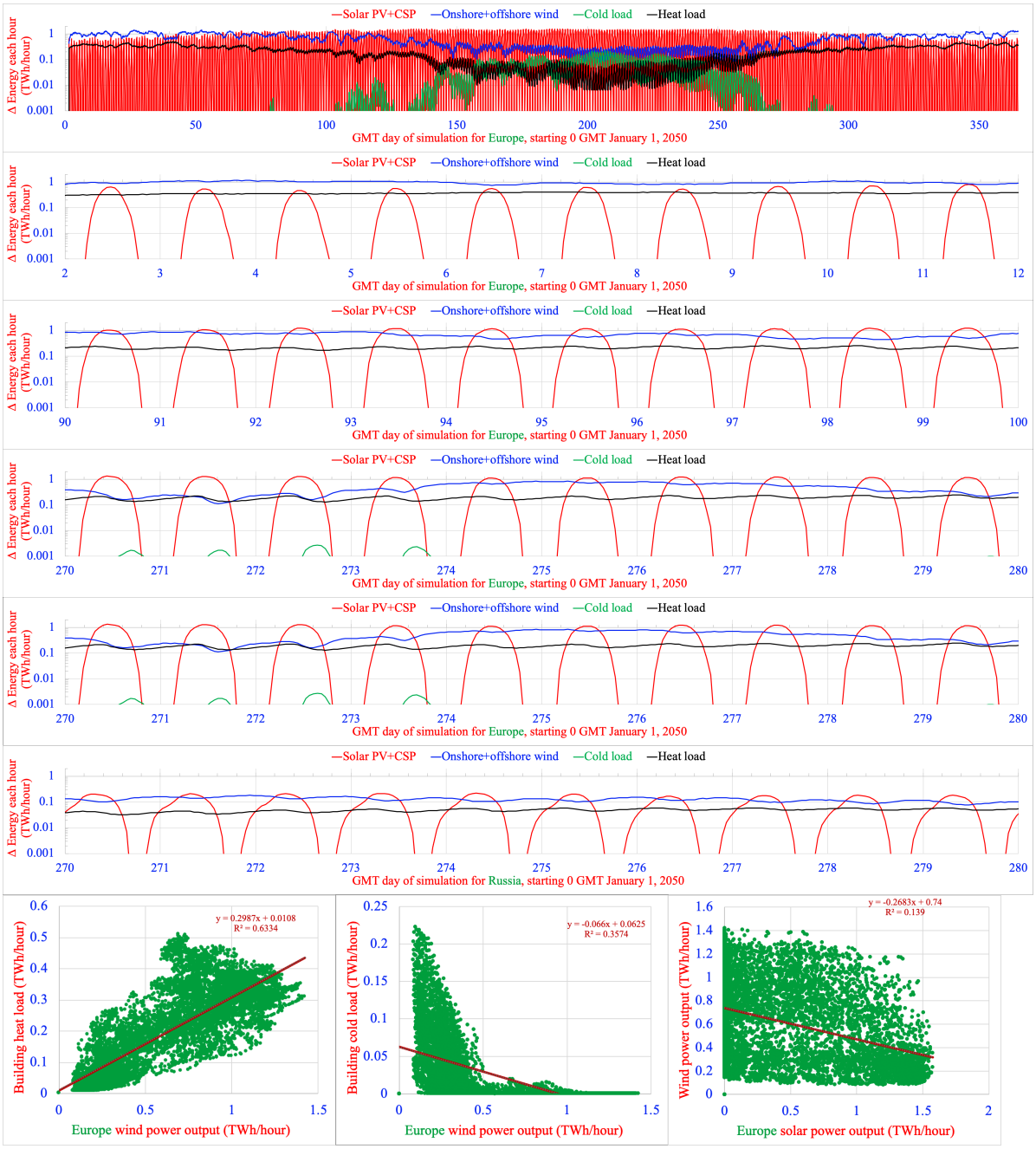
Solar PV+CSP
Onshore+offshore wind
Cold load
Heat load
Δ Energy each hour (TWh/hour)
GMT day of simulation for Europe, starting 0 GMT January 1, 2050
GMT day of simulation for Russia, starting 0 GMT January 1, 2050
Building heat load (TWh/hour)
Europe wind power output (TWh/hour)
y = 0.2987x + 0.0108
R² = 0.6334
Building cold load (TWh/hour)
y = -0.066x + 0.0625
R² = 0.3574
Wind power output (TWh/hour)
Europe solar power output (TWh/hour)
y = -0.2683x + 0.74
R² = 0.139

RUSSIA

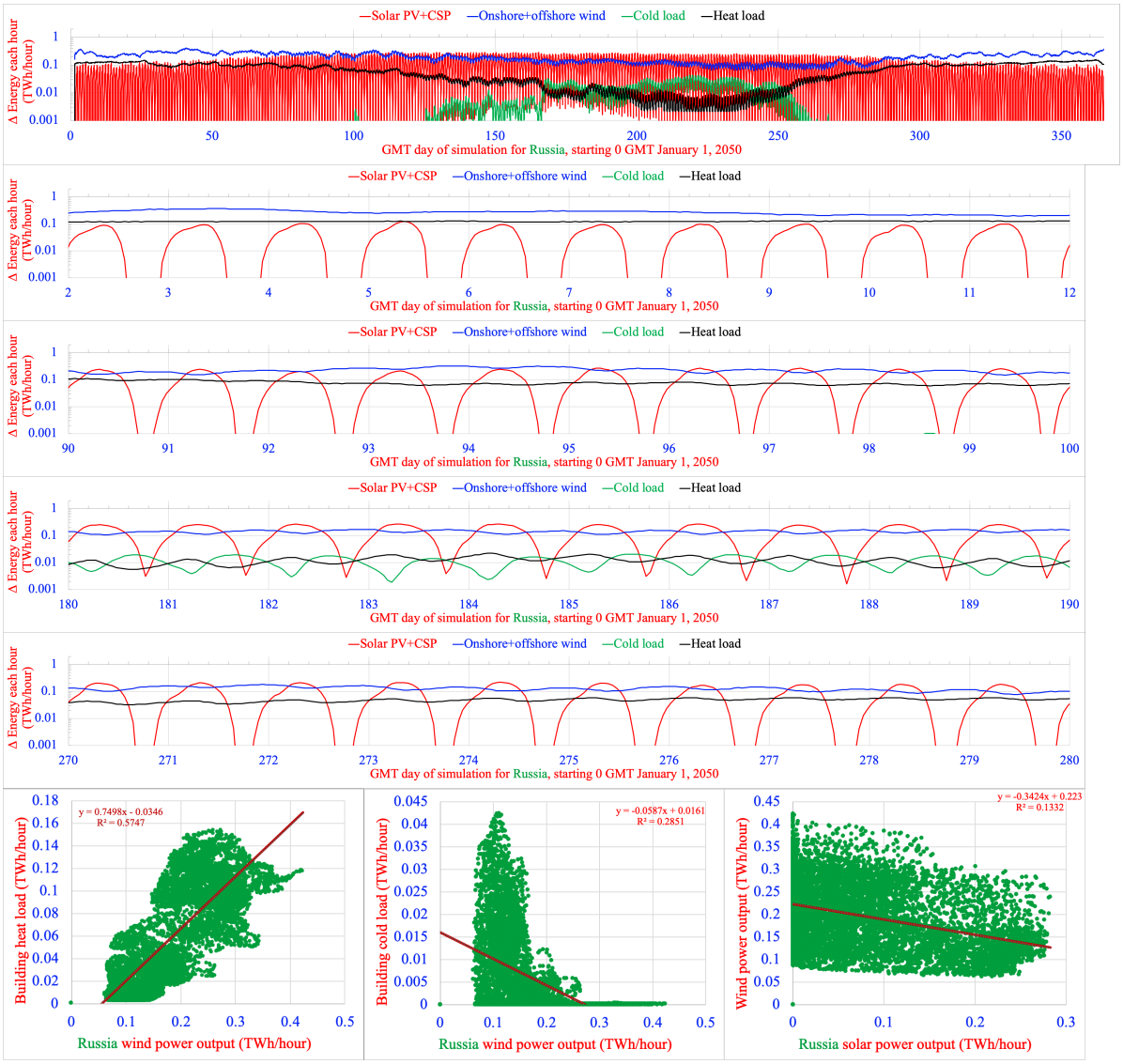
—Solar PV+CSP —Onshore+offshore wind —Cold load —Heat load
Δ Energy each hour (TWh/hour)
GMT day of simulation for Russia, starting 0 GMT January 1, 2050
Building heat load (TWh/hour)
y = 0.7498x - 0.0346
R² = 0.5747
Russia wind power output (TWh/hour)
Building cold load (TWh/hour)
y = -0.0587x + 0.0161
R² = 0.2851
Russia wind power output (TWh/hour)
Wind power output (TWh/hour)
y = -0.3424x + 0.223
R² = 0.1332
Russia solar power output (TWh/hour)

UNITED STATES

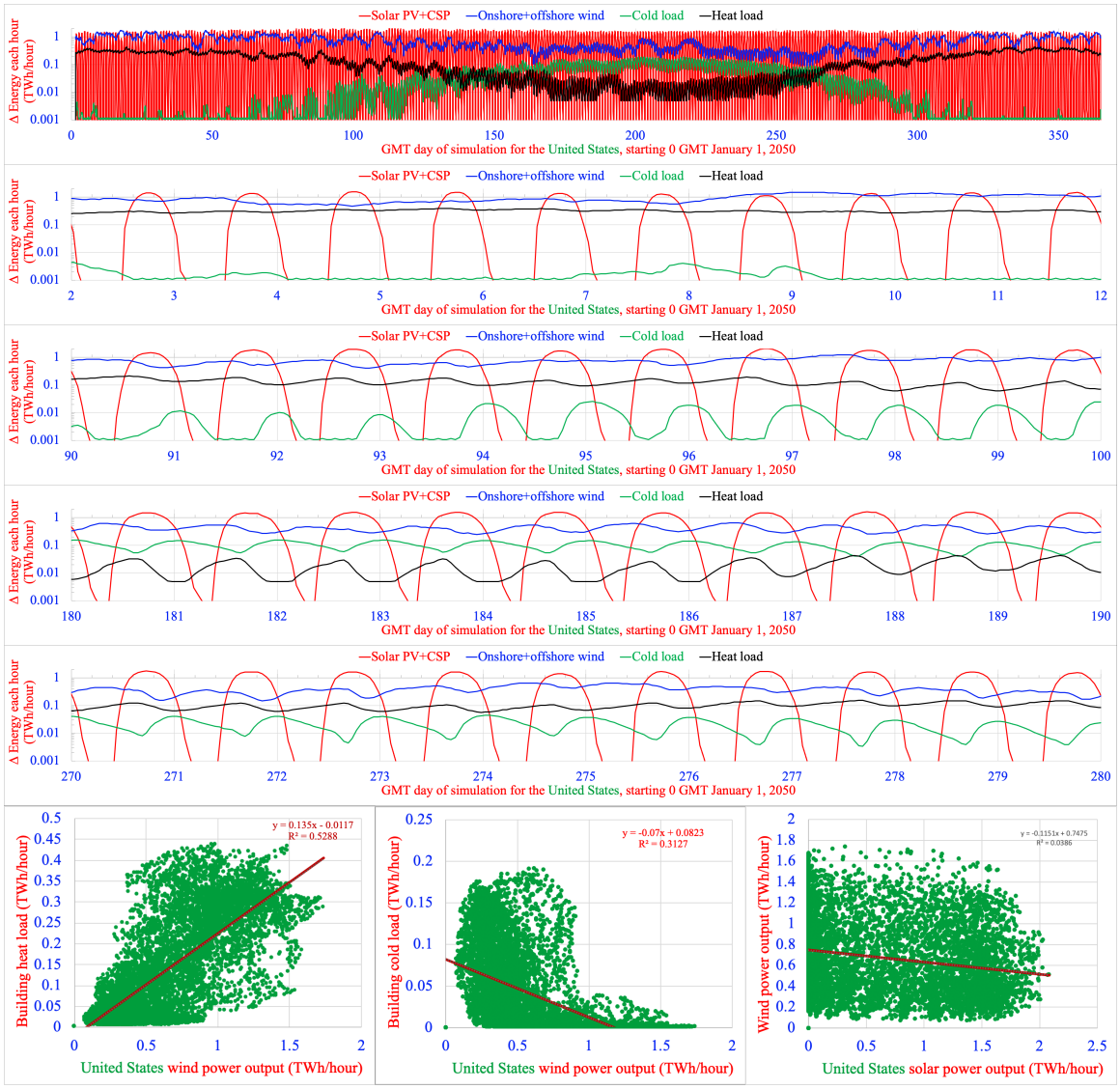

Figure S2. Time-series comparison, for 2050 and for 24 world regions, of LOADMATCH modeled WWS total power generation versus total load plus losses plus changes in storage plus shedding. The model was run at 30-s resolution. Results are shown hourly. No load loss occurred during any 30-s interval. Table S17 provides the budgets of the components of demand, generation, storage, and loss.

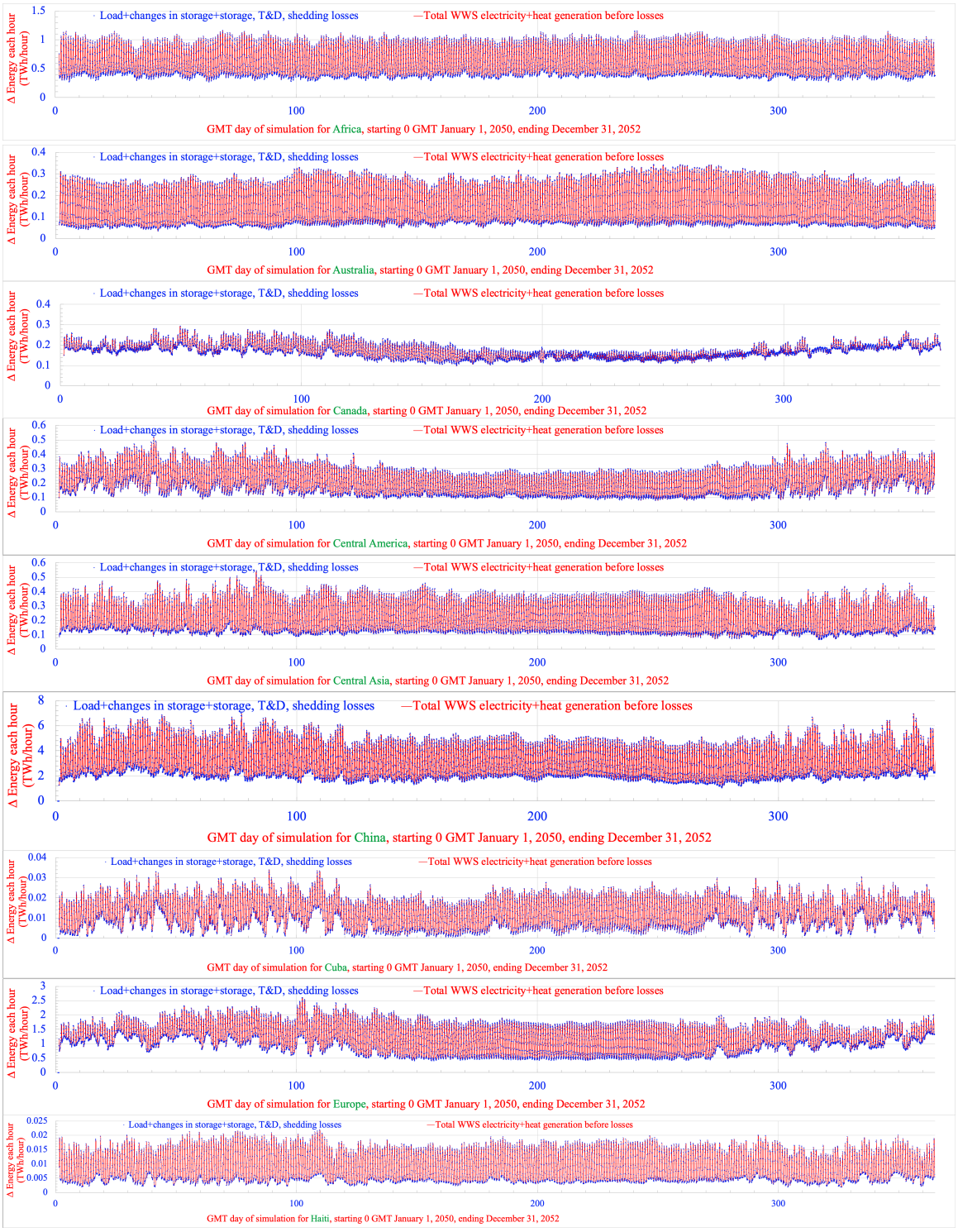

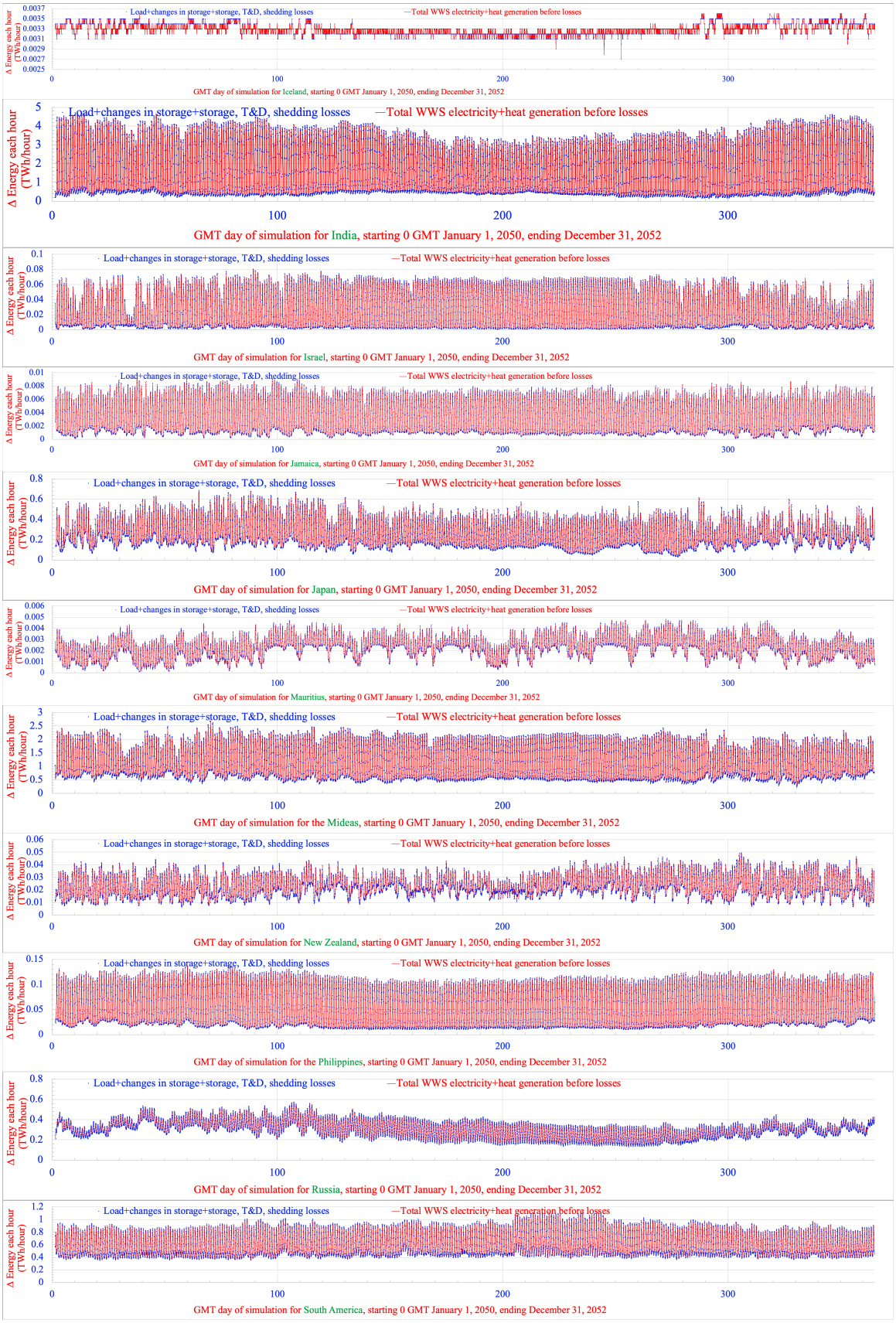
Load+changes in storage+storage, T&D, shedding losses
—Total WWS electricity+heat generation before losses
Δ Energy each hour (TWh/hour)
GMT day of simulation for Iceland, starting 0 GMT January 1, 2050, ending December 31, 2052
GMT day of simulation for India, starting 0 GMT January 1, 2050, ending December 31, 2052
GMT day of simulation for Israel, starting 0 GMT January 1, 2050, ending December 31, 2052
GMT day of simulation for Jamaica, starting 0 GMT January 1, 2050, ending December 31, 2052
GMT day of simulation for Japan, starting 0 GMT January 1, 2050, ending December 31, 2052
GMT day of simulation for Mauritius, starting 0 GMT January 1, 2050, ending December 31, 2052
GMT day of simulation for the Mideas, starting 0 GMT January 1, 2050, ending December 31, 2052
GMT day of simulation for New Zealand, starting 0 GMT January 1, 2050, ending December 31, 2052
GMT day of simulation for the Philippines, starting 0 GMT January 1, 2050, ending December 31, 2052
GMT day of simulation for Russia, starting 0 GMT January 1, 2050, ending December 31, 2052
GMT day of simulation for South America, starting 0 GMT January 1, 2050, ending December 31, 2052

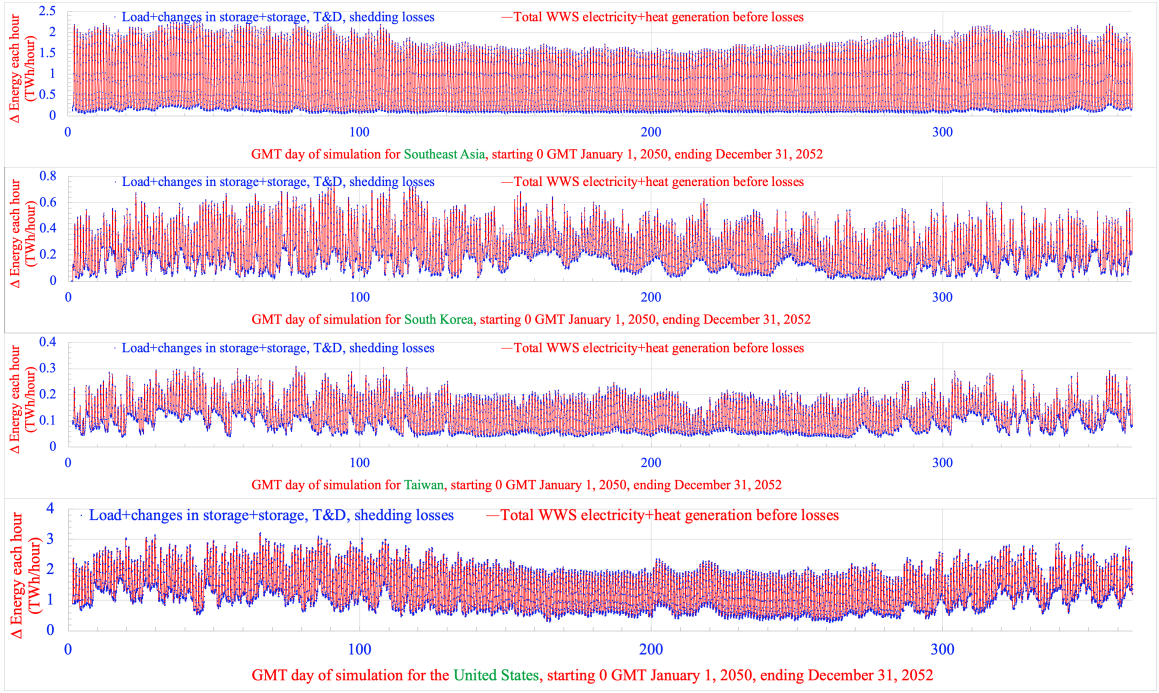
Load+changes in storage+storage, T&D, shedding losses
—Total WWS electricity+heat generation before losses
Δ Energy each hour (TWh/hour)
2.5
2
1.5
1
0.5
0
0
100
200
300
GMT day of simulation for Southeast Asia, starting 0 GMT January 1, 2050, ending December 31, 2052
Load+changes in storage+storage, T&D, shedding losses
—Total WWS electricity+heat generation before losses
Δ Energy each hour (TWh/hour)
0.8
0.6
0.4
0.2
0
0
100
200
300
GMT day of simulation for South Korea, starting 0 GMT January 1, 2050, ending December 31, 2052
Load+changes in storage+storage, T&D, shedding losses
—Total WWS electricity+heat generation before losses
Δ Energy each hour (TWh/hour)
0.4
0.3
0.2
0.1
0
0
100
200
300
GMT day of simulation for Taiwan, starting 0 GMT January 1, 2050, ending December 31, 2052
Load+changes in storage+storage, T&D, shedding losses
—Total WWS electricity+heat generation before losses
Δ Energy each hour (TWh/hour)
4
3
2
1
0
0
100
200
300
GMT day of simulation for the United States, starting 0 GMT January 1, 2050, ending December 31, 2052

Supporting References

S1. Jacobson, M.Z., Delucchi, M.A., Cameron, M.A., Coughlin, S.J., Hay, C., Manogaran, I.P., Shu, Y., and von Krauland, A.-K. (2019). Impacts of Green New Deal energy plans on grid stability, costs, jobs, health, and climate in 143 countries, *One Earth, 1*, 449-463.

S2. Jacobson, M.Z., Delucchi, M.A., Cameron, M.A. and Mathiesen, B.V. (2018). Matching demand with supply at low cost among 139 countries within 20 world regions with 100 percent intermittent wind, water, and sunlight (WWS) for all purposes. *Renewable Energy*, *123*, 236-248.

S3. De Stercke, S. (2014). Dynamics of Energy Systems: a Useful Perspective. IIASA Interim Report No. IR-14-013, International Institute for Applied Systems Analysis, IIASA, Laxenburg, Austria.

S4. Enevoldsen, P., and M.Z. Jacobson (2021). Data investigation of installed and output power densities of onshore and offshore wind turbines worldwide, *Energy for Sustainable Development*, 60, 40-51.